Acquisition and Description of Mariner 10 Television Science Data at Mercury

G. EDWARD DANIELSON, JR., AND KENNETH P. KLAASEN

Jet Propulsion Laboratory, Pasadena, California 91103

JAMES L. ANDERSON

California Institute of Technology, Pasadena, California 91125

The Mariner 10 television science subsystem was an improved version of the Mariner 9 system, using 1500-mm-focal-length optics. An elaborate picture-taking sequence resulted in transmission of over 4000 frames back to earth during two flyby encounters with Mercury. These sequences utilized a real-time data rate of 117.6 kbit/s, resulting in coverage of about 75% of the lighted portion of Mercury's surface at a resolution of better than 2 km. The complete set of useful images, which amounted to about 3000 frames, was processed with three different types of digital image-processing enhancements.

INTRODUCTION

The Mariner 10 spacecraft encountered the planet Mercury for the first time on March 29, 1974. Closest approach occurred on the dark side of the planet at an altitude of about 700 km. A second encounter occurred on September 21, 1974. The aim point for this flyby was chosen to be on the bright side at a range of about 50,000 km and about 45° south of the equatorial plane. The spacecraft carried twin, long focal length television cameras to photograph the surface of Mercury. About 3000 scientifically useful pictures were returned from both encounters with surface resolution of up to 120 m. About 40% of the surface of Mercury was photographed at better than 2-km resolution.

CAMERA CHARACTERISTICS

The Mariner 10 television science subsystem is similar in many respects to its predecessor on Mariner 9, which so successfully mapped the surface of Mars. One of the major differences was the optics. In order to increase the high-resolution coverage on the chosen flyby trajectory [*Dunne*, 1974] the focal length of the Mariner 10 telescope was increased to 1500 mm, 3 times that of the Mariner 9 high-resolution telescope. An auxiliary, wide-angle (50-mm focal length) optical system, accessed through the filter wheel, was added as well. A detailed description of the optical design, illustrated in Figure 1, is given by *Larks* [1974].

The sensor was an improved version of the selenium sulfur photosurface slow-scan vidicon. The electronic design was improved to reduce the camera's susceptibility to random electronic noise. A significant design change which resulted in an improvement over Mariner 9 was the incorporation of light flooding (F. Vescelus, unpublished data, 1975), which solved the residual image problem that had plagued earlier Mariner television data reduction, especially on Mariner 6, 7, and 9 [*Young*, 1974].

The system spectral transmission characteristics are shown in Figure 2. The optics spectral transmission is plotted with the spectral transmission for each filter. The complete system spectral response (in amperes per unit area of vidicon surface) for each filter has been calculated for an illuminating source with Mercury's spectrum, as published by *McCord and Adams* [1972]. The response curves have been normalized and plotted in Figure 3. The relative filter factors (ratio of integrated system spectral response without any filter to that with a given filter) for each filter are listed in Table 1 for each camera, for input radiances with both solar and mercurian spectra.

A detailed summary of all of the functional characteristics of the cameras is given below.

Characteristic	Value
Focal length	1500 mm
f/number	*f*/8.4
Field of view	0.36° × 0.48°
Scanned area	9.6 × 12.35 mm
Format	700 × 832 pixels
Encoding level	8 bits
Frame time	42 s
Resolution per TV line	9.5×10^{-6} rad

PICTURE NUMBERING AND DATA TRANSMISSION

Each Mariner 10 picture was assigned a unique identification number. The on-board electronic logic in the flight data subsystem (FDS) began numbering frames starting on the launch pad about 6 hours before lift-off. The numbers incremented by one for each successive 42-s frame. The FDS always assigned A camera frames odd numbers and B camera frames even numbers. Several times in flight, spacecraft anomalies caused the counter in the FDS to reset itself to zero. (One reset happened just as the spacecraft went into solar occultation at Mercury encounter. Thus the incoming pictures have been uniquely separated from those taken on the outgoing leg of the trajectory at the first Mercury encounter. Around closest approach the numbers are 274XX on the incoming side and 40–200 on the outgoing side.) However, any picture can be uniquely identified (to the National Space Science Data Center, for example) by stating the major target body along with the FDS number (e.g., earth FDS 14553 or Mercury FDS 48).

The Mariner 10 spacecraft could handle data in several modes. Data were recorded automatically on the on-board tape recorder and played back at a slower rate (22.05 kbit/s) as much as possible. Since the tape recorder took 2.24 hours to play back 36 pictures at this rate and surface resolution changed at a rate of about 0.8 km/h, full-disk, high-resolution coverage near Mercury encounter could not be accomplished by using this mode. Thus the pictures near closest approach

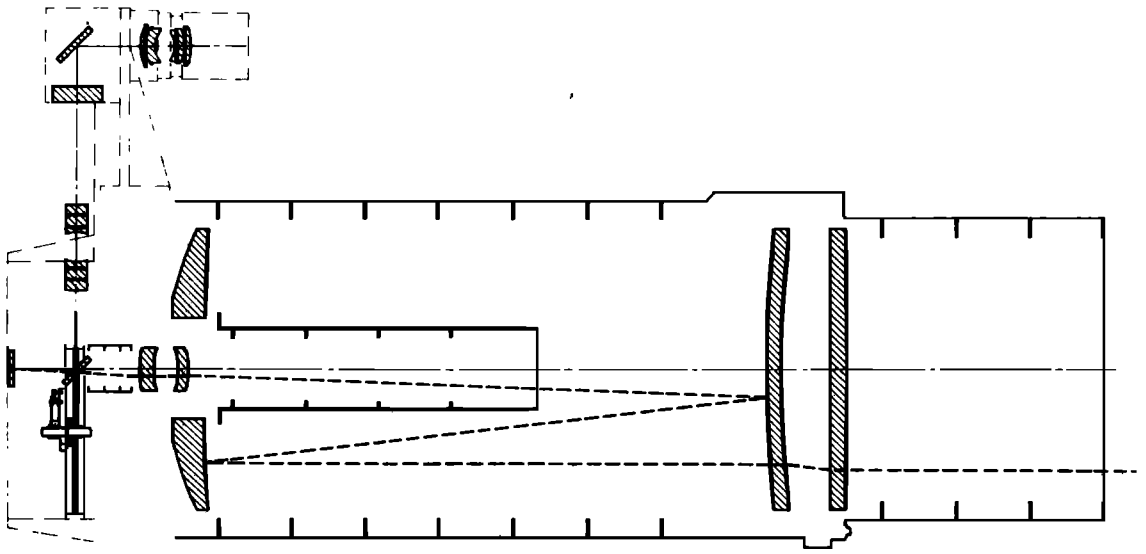

Fig. 1. Optical schematic of Mariner 10 high-resolution television subsystem.

were sent back in real time at 117.6 kbit/s (i.e., one picture transmitted every 42 s with no intermediate storage) but with a correspondingly noisier signal. During the mission this trade off between data rate and noise could be made independently of the other science data, since those data were telemetered in an independent telemetry channel. A third mode of data return was transmission in real time at 22.05 kbit/s. This slower, real-time data rate allowed only about one fifth of the total picture data to be returned for each frame. Two edit modes were available to select the data to be returned. In one, only the center strip (one quarter of the frame wide) was returned. In the other, called the skip-slide mode, only every fourth pixel in a line was returned, with the first pixel returned in a line being shifted over by two pixels from the previous line. In both of these edit modes the data were encoded with only 6 bits.

SEQUENCE

A summary of the imaging sequence for the first Mercury encounter is shown in Table 2.

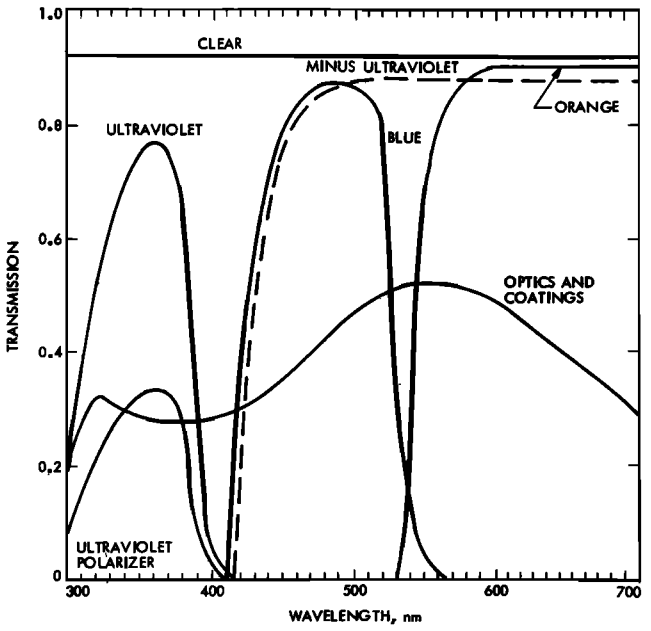

Fig. 2. Spectral transmission of Mariner 10 television subsystem optics and spectral filters in percent plotted as a function of wavelength.

Far Encounter

The incoming far-encounter sequence began as soon as Mercury could be viewed within the camera-pointing constraints of the spacecraft. The primary objectives of the far-encounter sequence were (1) to obtain imagery of Mercury at progressively better resolution while approaching the planet and (2) to check out and calibrate the television subsystem and the telemetry link.

The intent of the initial sequence 6 days prior to encounter was to photograph Mercury through each spectral filter at a minimum of two different exposure levels (five levels for the clear filter) in order to verify system sensitivity as a function of exposure over the dynamic range of the instrument. Scan platform pointing offsets and motion of the spacecraft within its attitude control dead band resulted in obtaining only about one-half the desired number of exposure levels (Table 3). Therefore a complete determination of the system response over the entire dynamic range was not possible. Enough data were obtained, however, to allow revised exposure calculations. The sequences on subsequent days consisted of imagery through all filters at midscale exposure levels and at progressively better resolution. After flying by Mercury on the

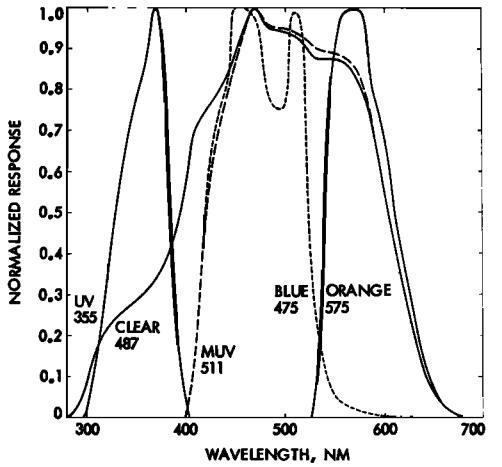

Fig. 3. Integrated optics, filters, and vidicon system response independently normalized for each spectral filter on the basis of the absolute Mercury spectrum and plotted as a function of wavelength.

TABLE 1. Mariner 10 Relative Filter Factors

Filter	Solar Radiance		Mercurian Radiance	
	A Camera	B Camera	A Camera	B Camera
Clear (CLR)	1.08	1.08	1.08	1.08
Minus ultraviolet (MUV)	1.57	1.49	1.44	1.39
Ultraviolet polarizing (UVP)	43.93	54.23	60.25	75.02
Blue (BL)	2.64	2.46	2.66	2.48
Orange (OR)	5.37	5.66	4.17	4.47
Ultraviolet (UV)	11.63	13.70	16.01	19.05

TABLE 2. First Mercury Encounter Sequence

Phase	Range, km	Resolution, km	Frames	FDS Numbers
Incoming far encounter, −6 to −1 day	5,700,000–800,000	280–20	546	14339–25728
Incoming color mosaicking, −16 to −4 hour	635,000–100,000	14–3	162	25927–27104
Close encounter, −4 to +4 hours	100,000–5500	3–0.12	592	27207–27477 0–392
Outgoing color mosaicking, +4 to +16 hours	100,000–635,000	3–14	144	494–1354
Outgoing far encounter, +1 to +3 days	800,000–2,800,000	20–60	108	2055–2590 5996–6049
Satellite search, +1 to +3 days	1,000,000–3,500,000		627	3932–5418 8045–8106
Total			2179	

dark side a similar type of far-encounter sequence was performed, beginning about 1 day after closest approach. Both incoming and outgoing data were played back from the spacecraft tape recorder at 22.05 kbit/s and had a bit error rate of less than 1 in 1000 bits. Figure 4 shows examples of the view of Mercury 2 days before and 3 days after encounter.

Color Mosaicking

Between 4 and 16 hours before and after encounter, higher-resolution color photography of Mercury was obtained. Besides obtaining higher-resolution coverage at less than full disk the intent of this sequence was to isolate color differences (which suggest compositional differences) by using widely separated spectral filters (UV and orange (OR)) and to measure the degree of polarization of the reflected light (which gives information on soil particle sizes) using the UV and UVP (ultraviolet polarizing) filters. These data were also played back from the tape recorder at 22.05 kbit/s at the correspondingly low bit error rate. Table 4 lists the best-resolution coverage of the entire disk and the best-resolution photograph of some part of the disk obtained through each color filter for both the incoming and the outgoing views of Mercury. Figure 5 shows the 8.9-km-resolution incoming view taken through the OR filter and the 10.6-km outgoing view taken through the UV filter.

Close Encounter

Within about 4 hours of closest approach, continuous, real-time imaging of Mercury was achieved except for a 30-min gap around encounter, when the spacecraft was on the dark side of the planet. The objective of this portion of the sequence was to obtain the highest-resolution coverage of as much of Mercury as possible, including photography of the entire visible portion of the planet at a resolution of 1 km or better. The images were all taken through the CLR (clear) filter to minimize the required exposure time and thereby the smear in the pictures. The 117.6-kbit/s data rate was used, yielding full-frame, full-resolution pictures at an average bit error rate of about 1 in 40 [*Clarke and Evanchuk*, 1974]. Figure 6 shows the planned mosaic patterns and the resolution ranges for the first four real-time mosaics. The actual coverage was similar to the plan except that motion of the spacecraft within its attitude control dead band and scan platform pointing errors caused some gaps in the coverage, especially near the bright limb. The actual footprints of the two highest-resolution inbound and the two highest-resolution outbound mosaics are shown in Figure 7. The resolutions range from about 900 m (FDS 27415 and 125) down to 120 m for the first outbound picture (FDS 42). Eighteen of the highest-resolution inbound frames (FDS 27458–27475) and the 17 highest-resolution outbound frames (FDS 42–58) were recorded for later playback at very low bit error rates. Table 5 summarizes the pertinent geometric parameters associated with those pictures with a resolution of about 500 m or better. Figure 8 shows the planned coverage and resolution ranges for the last five real-time outbound mosaics. Again, the actual coverage resembled the plan except for a few gaps.

At about 1 day and 22 hours after closest approach a search for a satellite of Mercury was begun. Additional search data were taken around 2 days and 12 hours and 3 days and 22

TABLE 3. Number of Exposure Levels Obtained During Mercury 1 Calibration Sequence

Filter	Camera A	Camera B
CLR	2	2
MUV	2	3
UVP	0	1
BL	4	2
OR	1	1
UV	2	0

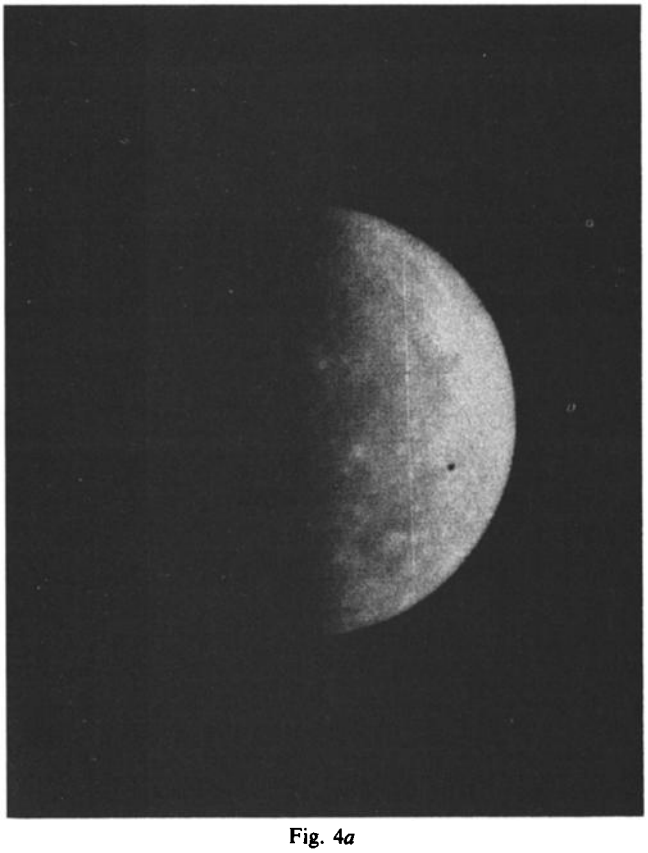

Fig. 4a

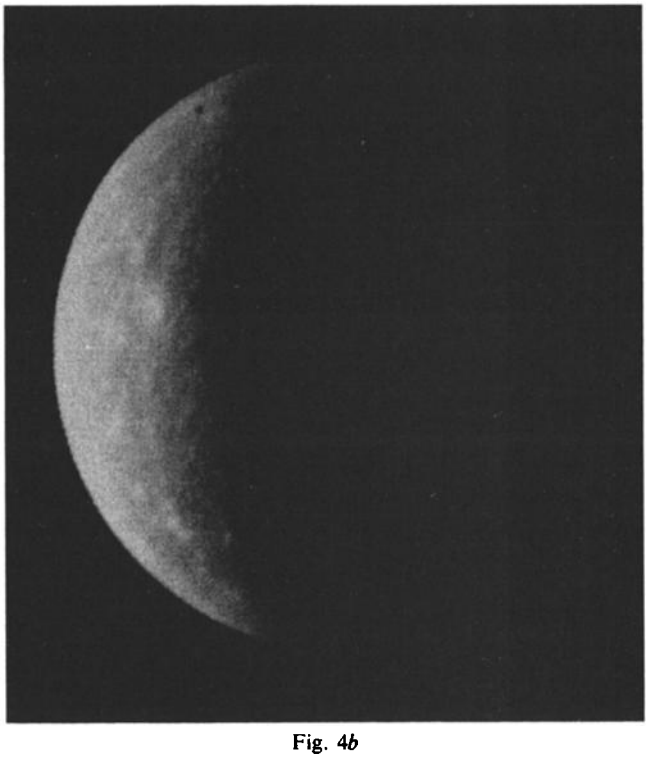

Fig. 4b

Fig. 4. The (right) incoming and (left) outgoing far-encounter views of Mercury.

hours after encounter. The 1d 22h sequence consisted of 521 frames taken with an 11.7-s exposure time and sent back in real time at 22.05 kbit/s, some being in the skip-slide edit mode and others in quarter-frame strips. The 2d 12h sequence contained 70 taped frames with 8.4-s exposures, and the 3d 22h sequence contained 35 taped frames with 11.7-s exposures. Each of these sequences covered an area out to about 36 Mercury radii on either side of the planet in the ecliptic plane and 12 Mercury radii above and below the ecliptic plane. Preliminary analysis of these data revealed no satellite larger than 5 km in diameter with an albedo similar to that of Mercury.

Second Mercury Encounter

A summary of the imaging sequence for the second Mercury encounter is shown in Table 6. Imaging began when Mercury could first be viewed by the camera. The main purpose of the far-encounter sequence was to check out and calibrate the television subsystem after its 6-month rest. The sequence 4 days prior to encounter included pictures of Mercury taken through each spectral filter of each camera at a midscale exposure level and sent back at 22.05 kbit/s in the skip-slide mode. The sequence 3 days before encounter was a rather extensive instrument calibration with several exposure levels through each filter spread over the dynamic range of each camera (Table 7). Since the television optics heaters were shorted out by a power system anomaly soon after Mercury 1 encounter, the camera operating temperature was much lower, and a recalibration of the instrument was required to verify exposure settings and for use in photometric analysis. Two days before encounter, images of Jupiter were taken at several exposure levels through the CLR filter to photometrically calibrate the instrument further. One day before and 1 day after closest approach, pictures were taken through each filter at a midscale exposure level and were transmitted in real time at 117.6 kbit/s. At these times the planet Mercury nearly filled the camera field of view. At about 3 hours before encounter, real-time imaging at 117.6 kbit/s began again and continued until about 3 hours after encounter. Photomosaics of the images taken during the Mercury 2 close encounter are shown in Figure 9 along with the areas of the planet planned to be covered by each mosaic. The intent of the close-encounter sequence was to cover the areas in the south polar and bright limb regions not photographed on Mercury 1. The Mercury 2 photography would then provide both a geologic and a cartographic tie between the two quadrants photographed on Mercury 1 and would yield a more representative sample of the surface morphology upon which to base scientific conclusions. The images were all taken through the CLR filter except for one wide-angle-filter (WAF) frame taken near closest

TABLE 4. Best Resolution of Color Mosaics

Filter	Incoming		Outgoing	
	Full Coverage, km	Partial Coverage, km	Full Coverage, km	Partial Coverage, km
OR	8.9	4.7	21.0	5.3
UV	7.8	7.8	10.6	6.3
UVP	21.0	7.8	21.0	7.4
BL	41.0	10.0	8.5	8.5
MUV	8.9	8.9	8.5	8.5

approach and the two frames on either side of the WAF frame, during which the filter wheel was stepping from CLR to WAF and back to CLR. The average bit error rate achieved was about 1 in 35. Resolution was between 1 and 2 km for the real-time images. Failure of the tape recorder prior to the encounter sequence precluded its use.

A third pass on the dark side of Mercury is scheduled for March 16, 1975. Although the dark side aim point was chosen to maximize the science return from the particles and fields experiments, valuable imaging science data can also be obtained. The planned imaging sequence consists of a far-encounter calibration and a check-out sequence followed by a close-encounter sequence of high-resolution photography aimed at targets of interest selected from earlier photography. Frames with resolution as high as 60 m are anticipated.

DATA PROCESSING

Standard computer digital image processing of all useful imaging data was performed by software developed for previous Mariner imaging subsystems with some modifications necessitated by hardware and picture-taking sequence differences. Some aspects of the development of Mariner image processing are described by *Rindfleisch et al.* [1971] and *Dunne et al.* [1971] in the context of Mariner 6 and 7. An image-processing system was developed at the Jet Propulsion Laboratory for Mariner 9, the principal features of which are elucidated by *Cutts* [1974]. This existing 'MTC/MTVS' image-processing and hard-copy production facility was chosen by the Mariner 10 project to perform the standard processing of all pictures. The standard processing for Mariner 10 was a two-part operation, consisting of 'real-time' processing and 'systematic' processing.

In real-time processing, about half of the images were reconstructed immediately upon receipt of the data in both volatile and hard-copy forms to support engineering and press release requirements. The volatile display was converted to standard 525-line television and distributed by video cable to monitors used by engineers and scientists and to other monitors for NASA guests in Pasadena, California, and Greenbelt, Maryland. Since this real-time processing system could not reconstruct the images as fast as data were received from the Goldstone tracking station and because overseas stations could not relay the data to Pasadena as fast as the spacecraft could send them, a second pass of all the data through the sys-

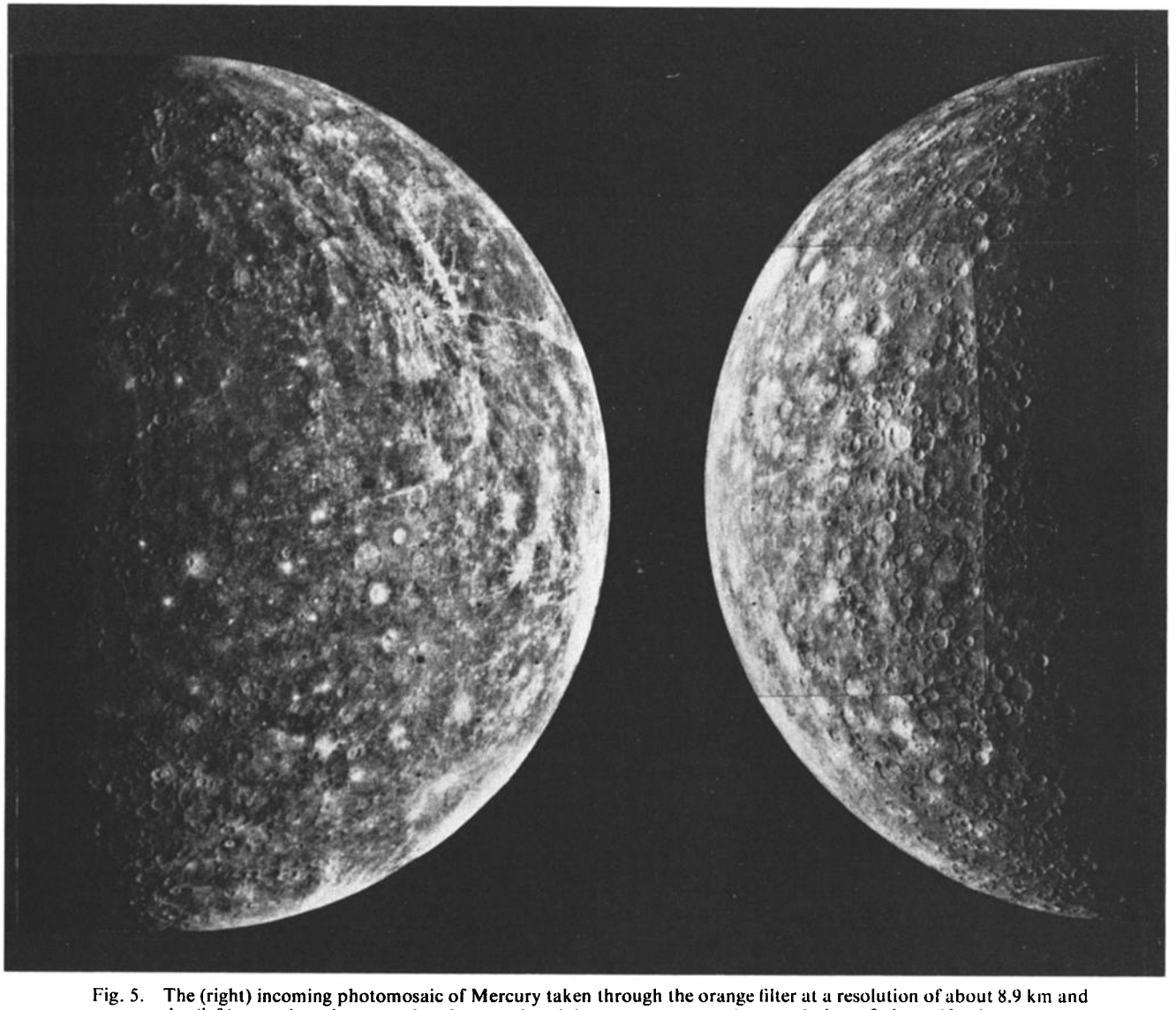

Fig. 5. The (right) incoming photomosaic of Mercury taken through the orange filter at a resolution of about 8.9 km and the (left) outgoing photomosaic taken at ultraviolet wavelengths with a resolution of about 10.6 km.

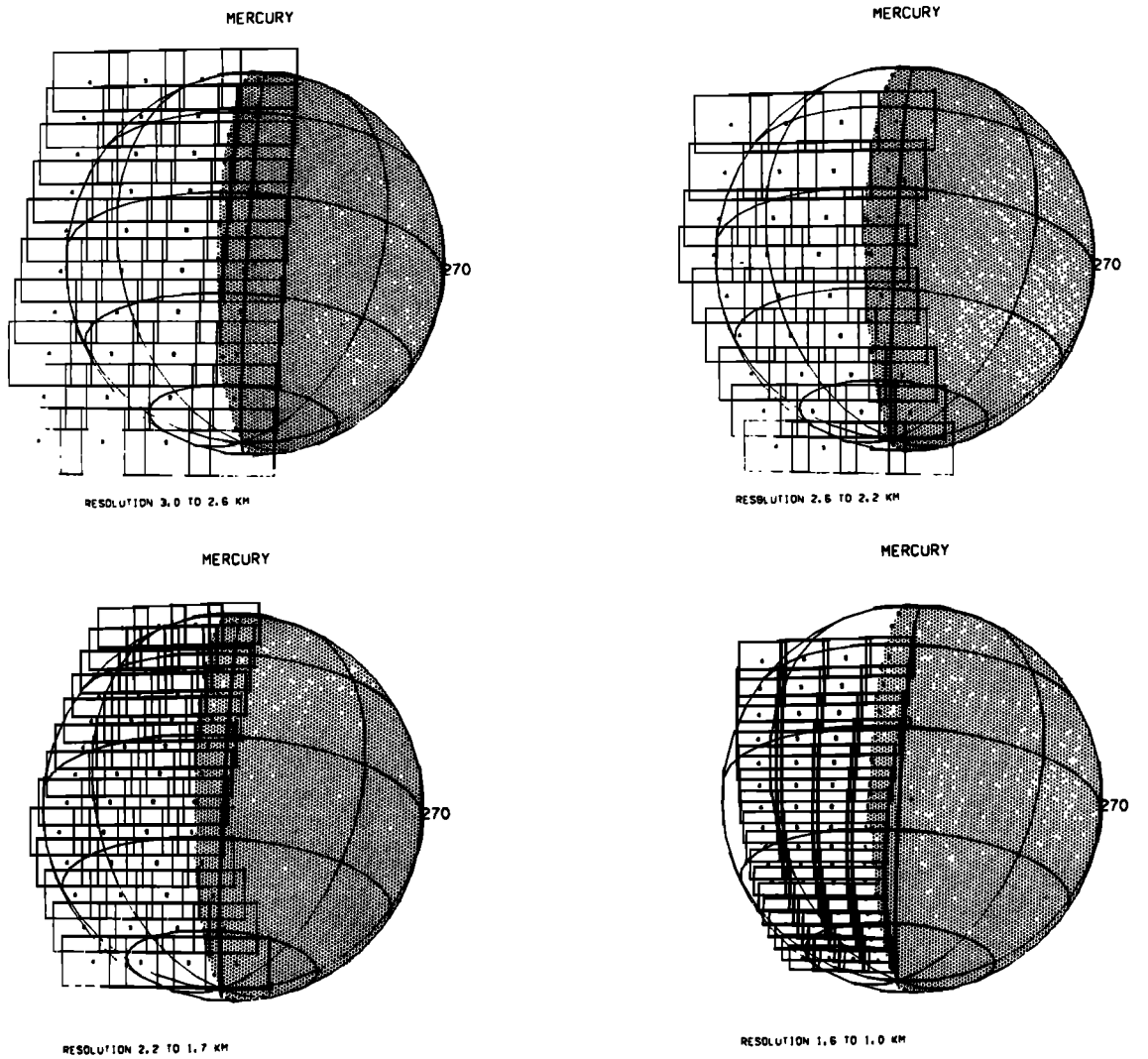

Fig. 6. Planned coverage of the first four real-time mosaics at the first Mercury encounter. The range of surface resolution is shown for each mosaic.

tem was necessary subsequent to the initial receipt. This pass was called systematic processing. In the process of production of the TV experimenters' data record (a reformatted magnetic tape version of the video data) a histogram of the distribution of raw brightness values in each frame was produced. Inspection of these histograms before reconstruction of the images in systematic processing permitted many frames showing only black sky or unilluminated planet to be excluded from reconstruction.

Three versions of each frame were produced in systematic processing: a contrast-enhanced 'raw' version and two spatially filtered versions designated 'high-pass-filtered' and 'vertical AGC,' the filtered versions differing the direction in the frame in which the filter was operating.

A 'filter' in image-processing terminology is the emphasis of some spatial frequency components of an image with respect to others. Most commonly, as is true in this case, the high-frequency components, which contain the fine detail of the image, are retained, while the lower-frequency components are suppressed. In the high-pass-filtered version the brightness value of each picture element is adjusted by removing a fraction of the average of picture elements nearby in the horizontal direction. In the vertical AGC version, picture elements are adjusted by a function of the picture elements above the one being adjusted.

The software system developed for Mariner 9 was modified principally to accommodate Mariner 10 data system hardware changes. The major changes from Mariner 9 to Mariner 10 were a reduction from 9 to 8 bits per picture element and the introduction of edited data modes for major parts of the mission. Changes in the text accompanying each image were necessitated by an inability to obtain timely target intercept information and a requirement to display engineering data for system test purposes.

Improvements were made in the limb-ringing suppression and reseau suppression algorithms used in the filtered versions. The bright limb of a planet represents the extreme case of high spatial frequency information and completely disrupts the operation of simple filters in its vicinity. To avoid this problem, which also occurs at frame edges, a routine is written that locates high-brightness edges at either side of each line and replaces values outside those edges with the average of a few picture elements just inside the edges. The reseaus, a grid of reflective spots on the vidicon faceplate for geometric calibration purposes, appear as very dark spots in the image and produce a similar problem for simple filter routines. After

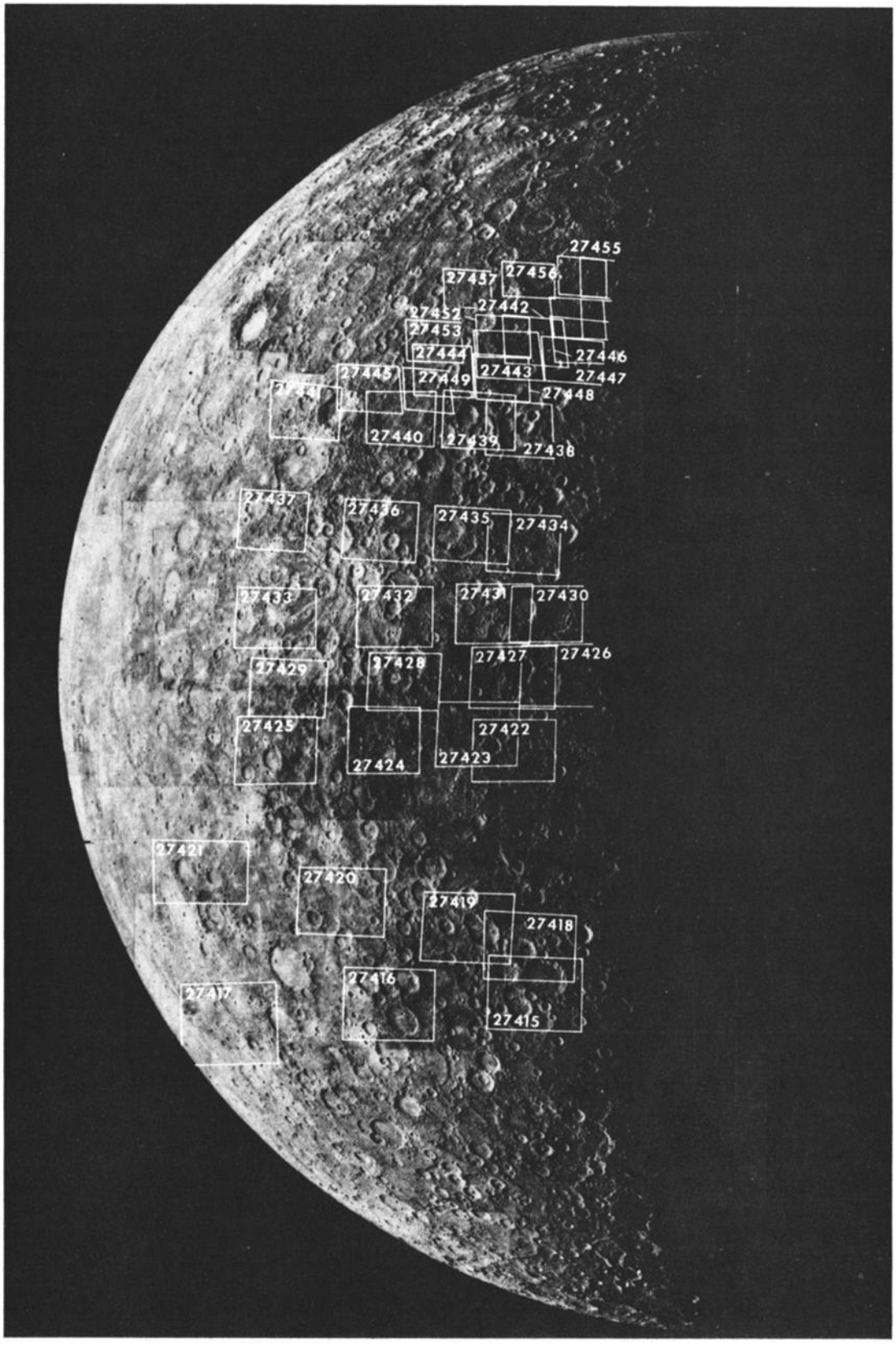

Fig. 7*a*

Fig. 7. Footprints of the highest-resolution (*a*, *b*) inbound and (*c*, *d*) outbound frames actually obtained. The FDS number for each frame is also shown. The footprints have been plotted on high-resolution (2 km) photomosaics of Mercury.

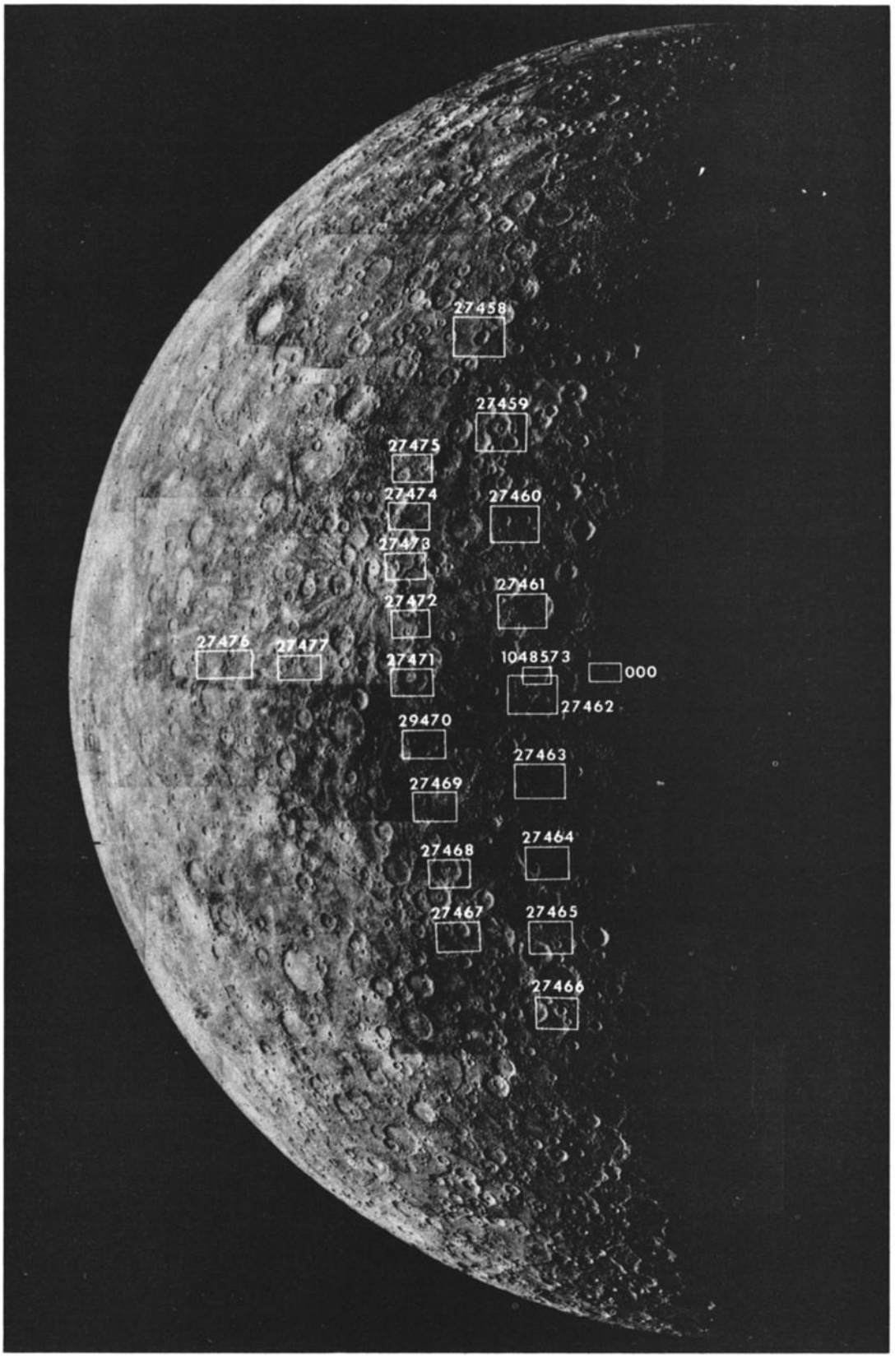
27458
27459
27475
27474
27460
27473
27461
27472
27476
27477
27471
1048573
000
27462
29470
27463
27469
27464
27468
27467
27465
27466

Fig. 7*b*

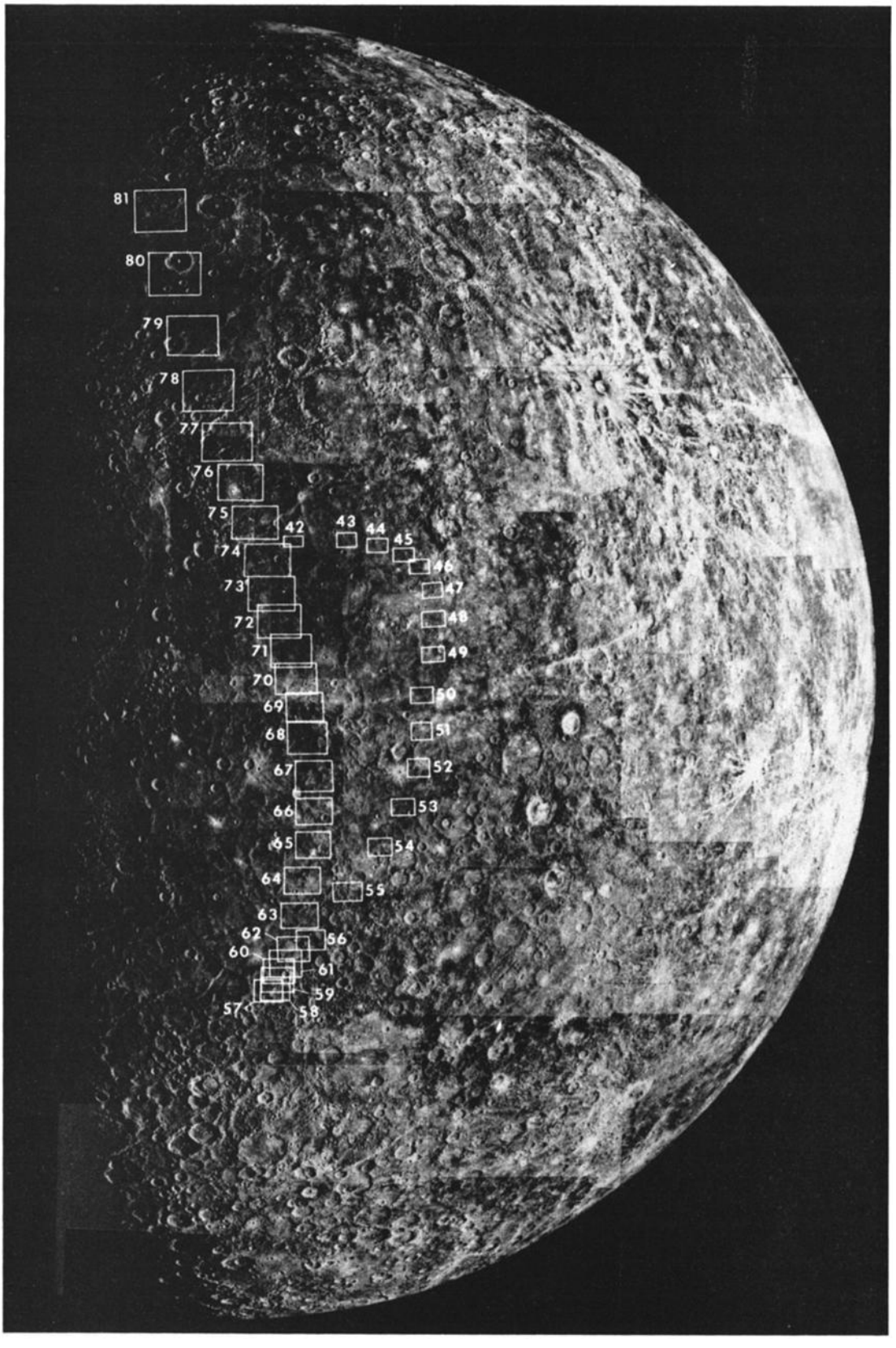
81
80
79
78
77
76
75
42
43
44
45
74
46
73
47
72
48
71
49
70
50
69
51
68
52
67
53
66
54
65
55
64
63
56
62
60
61
59
57
58

Fig. 7*c*

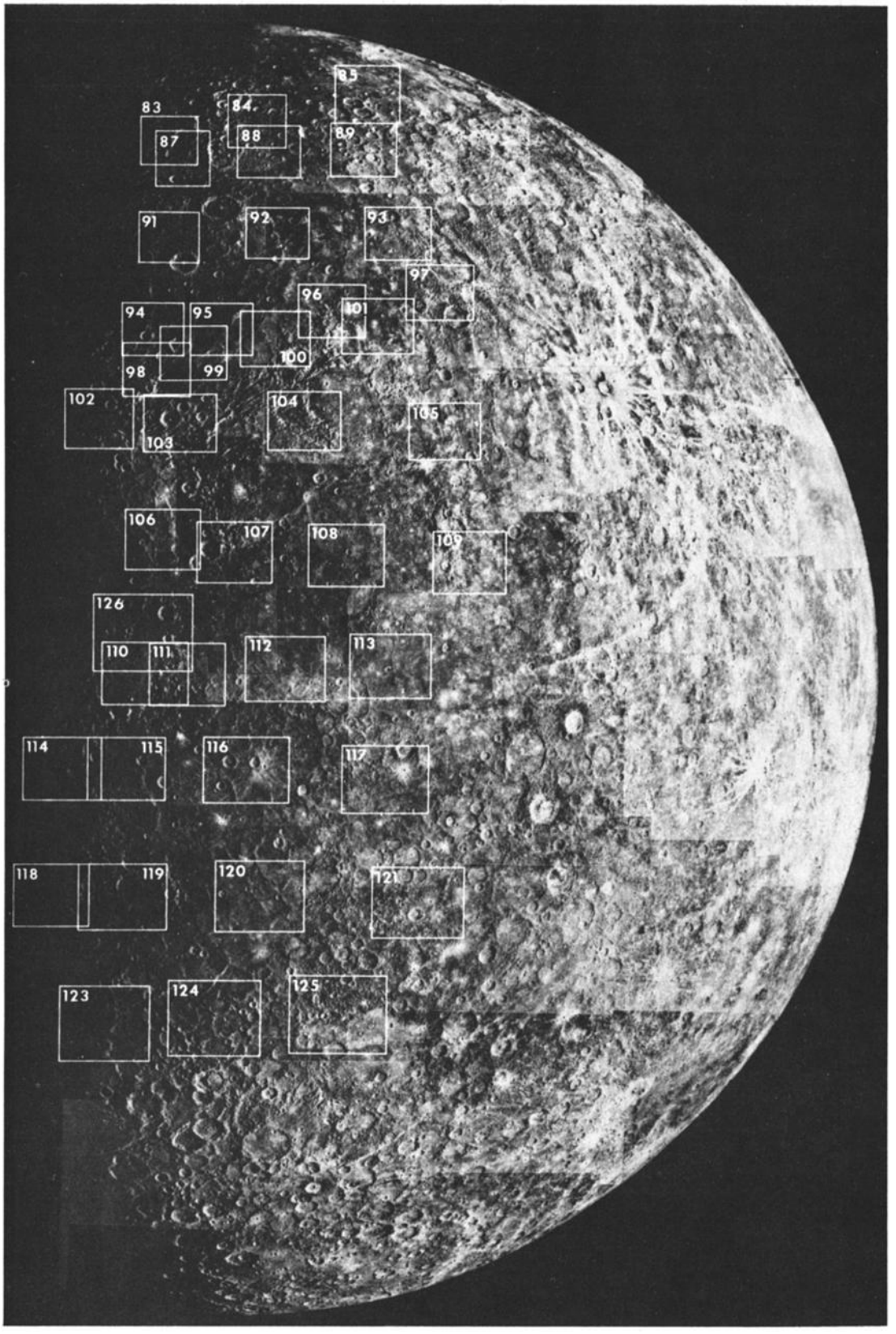
83
84
85
87
88
89
91
92
93
94
95
96
97
98
99
100
101
102
103
104
105
106
107
108
109
110
111
112
113
114
115
116
117
118
119
120
121
123
124
125
126

Fig. 7*d*

TABLE 5. Geometric Parameters for High-Resolution Frames

FDS No.	Latitude, deg	Longitude, deg	Slant Range, km	Incident Angle, deg	Emission Angle, deg	Phase Angle, deg	Frame Dimension, km		Resolution,* m
							Horizontal	Vertical	
27458	10.0	23.7	20,213	76	50	111	172	133	449
27459	−0.22	19.4	19,774	80	39	111	169	130	439
27460	−8.6	17.8	19,334	82	33	111	165	127	429
27461	−15.9	17.8	18,895	82	30	111	161	124	419
27462	−23.2	17.2	18,456	83	29	111	157	121	410
27463	−30.5	17.1	18,018	83	30	112	153	118	400
27464	−37.7	17.2	17,579	84	33	112	150	116	390
27465	−44.5	18.6	17,140	84	38	112	146	113	381
27466	−51.4	19.9	16,702	84	44	112	143	110	371
27467	−43.0	29.8	16,264	75	46	114	139	107	361
27468	−37.3	28.4	15,826	75	44	114	135	104	351
27469	−33.0	27.5	15,389	74	43	115	132	101	342
27470	−26.5	27.7	14,952	73	43	115	128	99	332
27471	−21.2	28.8	14,515	72	44	116	124	96	322
27472	−16.0	28.5	14,078	72	45	117	121	93	313
27473	−11.0	28.5	13,642	71	48	117	117	90	303
27474	−6.9	27.8	13,206	71	50	118	113	87	293
27475	−3.5	27.2	12,770	70	53	118	110	85	283
27476	−15.0	49.2	12,800	52	69	121	107	83	284
27477	−18.0	40.0	12,100	61	60	121	101	81	269
1048575	−21.5	15.9	11,500	84	37	121	96	79	255
000	−20.0	11.9	11,000	88	33	121	92	77	244
42	31.5	166.0	5,468	70	45	110	43	33	121
43	31.8	160.5	5,873	66	48	109	46	36	130
44	30.2	158.5	6,276	64	48	107	50	38	139
45	29.0	156.8	6,696	62	47	106	53	41	149
46	28.0	156.0	7,119	61	46	104	57	44	158
47	26.0	155.0	7,545	59	46	103	60	46	167
48	22.8	155.5	7,959	59	44	102	64	49	177
49	19.8	156.0	8,385	59	42	100	67	52	186
50	16.5	156.5	8,822	59	41	99	71	55	196
51	12.8	157.	9,273	58	40	98	74	57	206
52	10.5	157.4	9,724	58	40	97	78	60	216
53	7.7	160.0	10,163	61	37	96	82	63	226
54	3.5	162.5	10,633	63	37	94	85	66	236
55	0.8	164.5	11,098	65	36	93	89	68	246
56	−4.0	168.0	11,607	68	37	92	92	71	258
57	−8.0	171.8	12,121	72	38	90	96	74	269
58	−7.9	171.5	12,554	72	38	90	100	77	279
59	−6.6	171.0	12,960	72	36	89	103	80	288
60	−5.8	171.0	13,378	72	35	89	107	82	297
61	−4.7	169.8	13,796	70	34	89	111	85	306
62	−4.0	169.7	14,300	70	34	88	114	88	317
63	−1.3	169.6	14,694	69	31	88	118	91	326
64	2.2	169.1	15,074	69	28	88	122	94	335
65	5.6	167.8	15,258	68	25	88	125	97	339
66	8.2	167.1	15,874	68	24	87	129	99	352
67	10.9	167.1	16,289	68	22	87	133	102	362
68	14.3	167.4	16,686	69	19	86	136	105	370
69	16.9	167.1	17,113	69	18	86	140	108	380
70	19.7	167.5	17,536	69	17	86	144	111	389
71	22.0	168.3	17,962	70	15	85	147	114	399
72	25.5	169.0	18,398	72	15	85	150	116	408
73	27.2	169.2	18,839	72	15	85	154	119	418
74	31.1	169.3	19,300	73	17	84	158	122	428
75	33.6	170.1	19,755	74	18	84	162	125	439
76	37.1	171.3	20,223	76	21	84	166	128	449
77	40.8	172.5	20,707	77	24	83	170	131	460
78	46.0	172.8	21,235	78	29	83	172	133	471
79	49.7	175.9	21,738	81	32	82	176	136	483
80	57.7	178.2	22,374	84	41	82	180	139	497
81	64.9	181.3	23,024	87	48	82	184	142	511

Geometric parameters have been referenced to center of frame.
* Has been defined to be 2.2 TV lines.

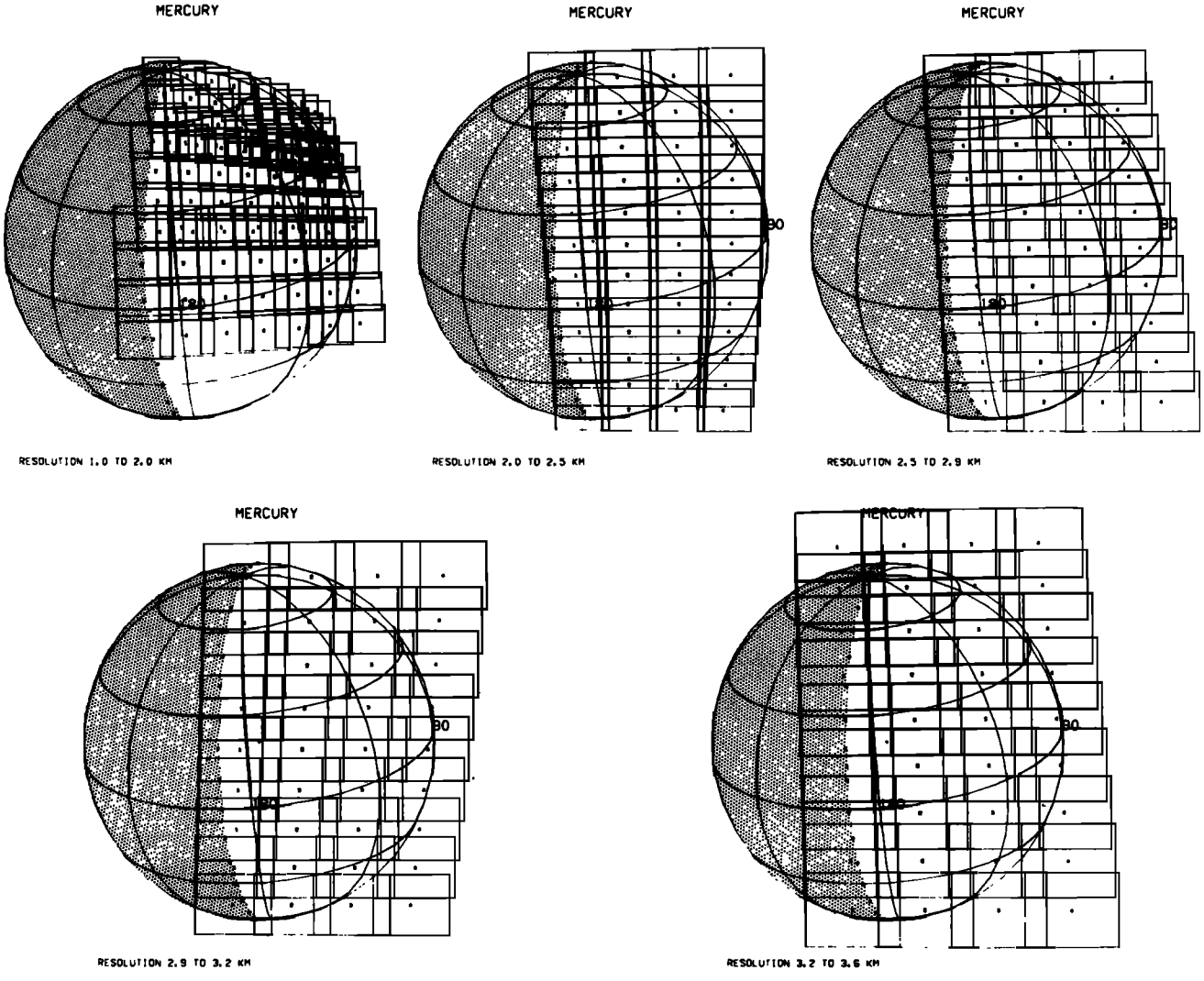

Fig. 8. Planned coverage of the last five real-time mosaics at the first Mercury encounter. The range of surface resolution is shown for each mosaic.

TABLE 6. Second Mercury Encounter Sequence

Phase	Range, km	Resolution	Frames	FDS Numbers
Incoming far encounter, −4 to −1 day	3,800,000–900,000	160–20	433	158495–160760 164607–164734
Jupiter calibration photography, −2 day	7.1×10^8	16,000	44	162632–162677
Close encounter, −3 to +3 hours	120,000–50,000	2.6–1.1	360	166471–167033
Outgoing far encounter, +1 day	900,000	20	72	168765–168848
Total			909	

dark areas at the edges of lines are replaced for limb-ringing suppression, reseaus are suppressed by replacing remaining low-brightness values with the average of those near them.

Significant changes for Mariner 10 included disabling the limb-ringing suppression algorithm on the dark side of frames containing a significant fraction of near-terminator scene information and modifying the automatic contrast enhancement of the raw version of the same frames to avoid suppressing useful low-brightness scene information. The result of

TABLE 7. Number of Exposure Levels Obtained During Mercury 2 Calibration Sequence

Filter	Camera A	Camera B
CLR	6	7
MUV	4	2
UVP	2	2
BL	4	4
OR	5	2
UV	2	5

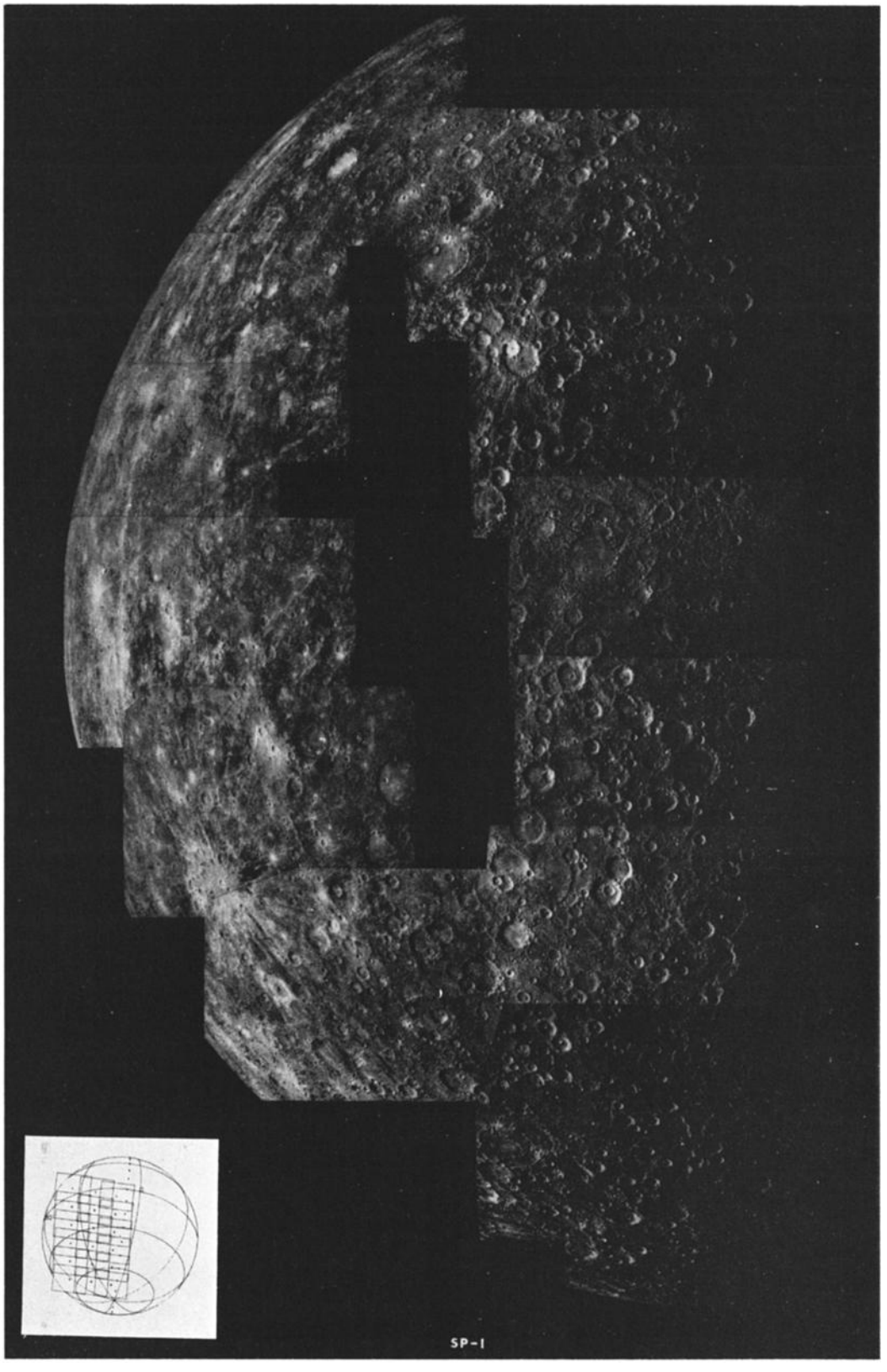

Fig. 9*a*

Fig. 9. Photomosaics of frames taken during the second Mercury encounter. Areas of planned coverage are shown as well.

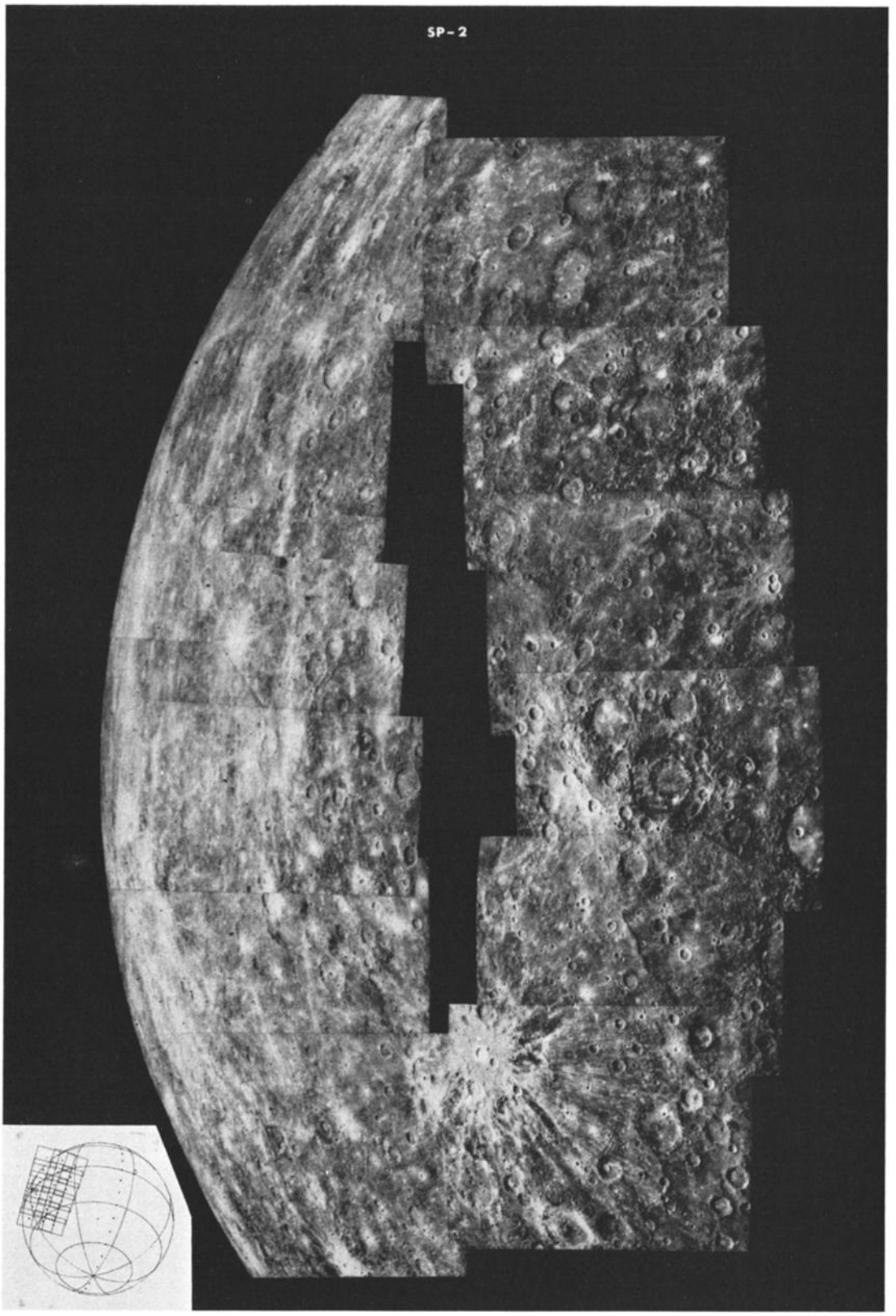

Fig. 9*b*

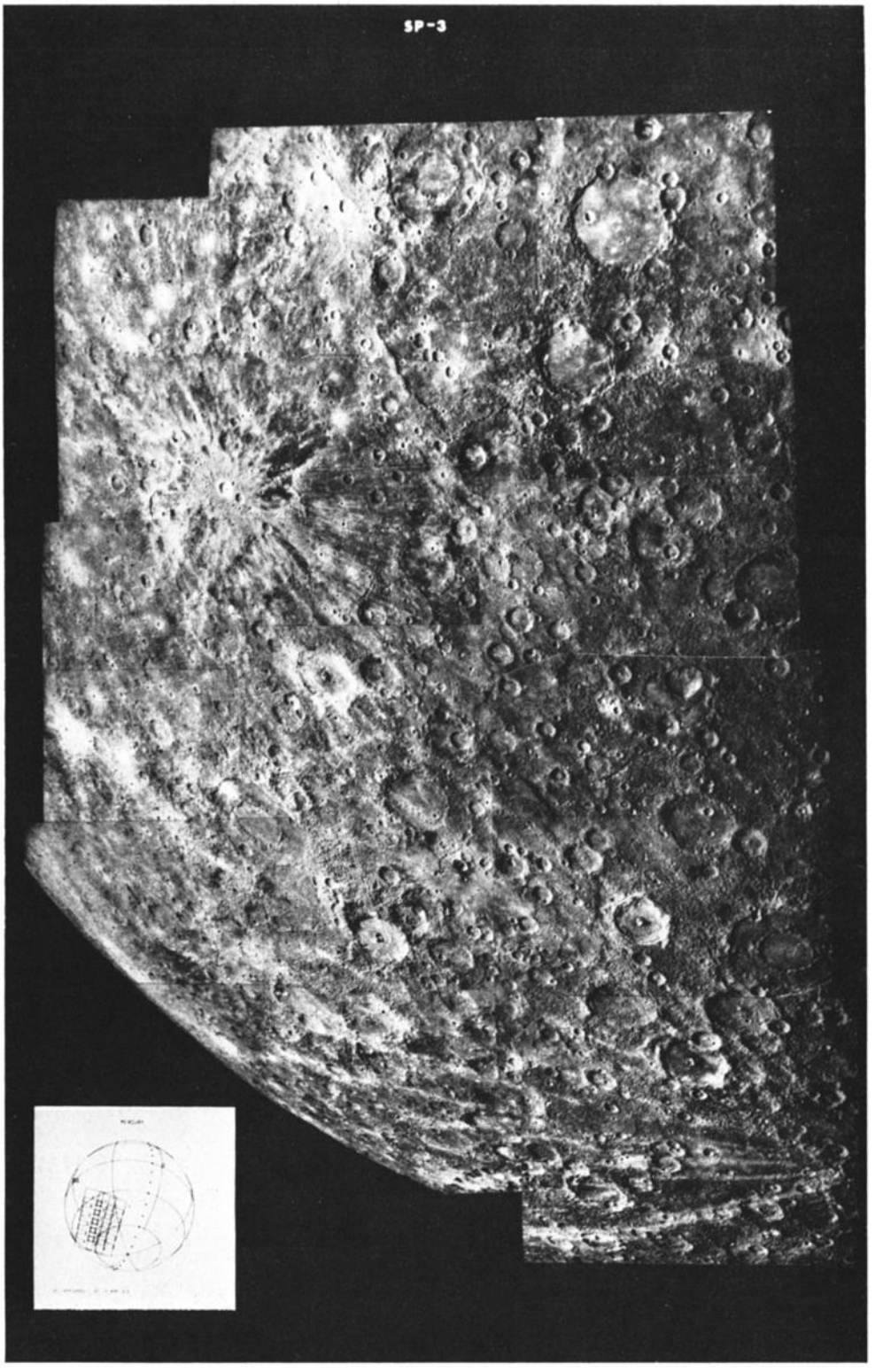

Fig. 9c

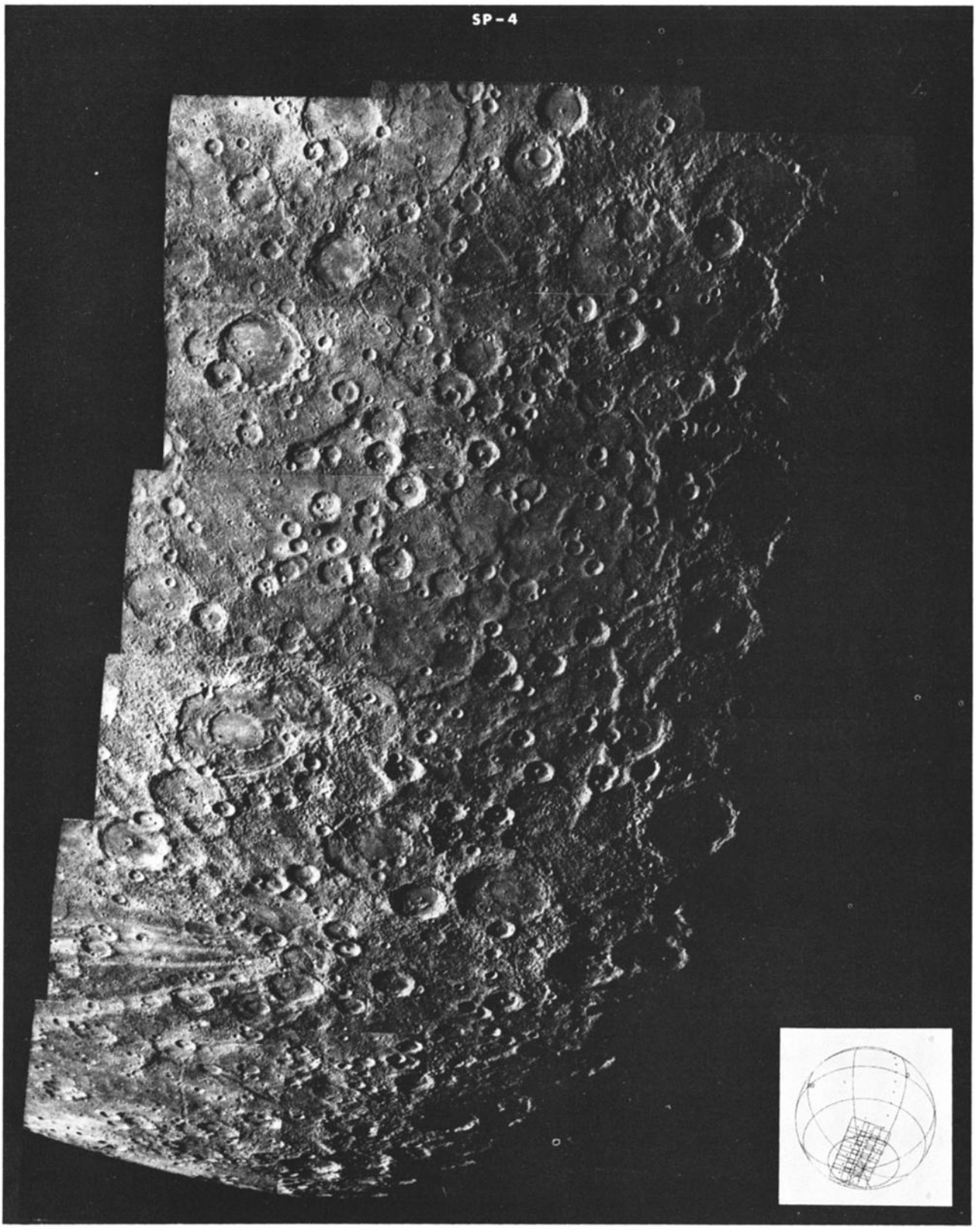

Fig. 9*d*

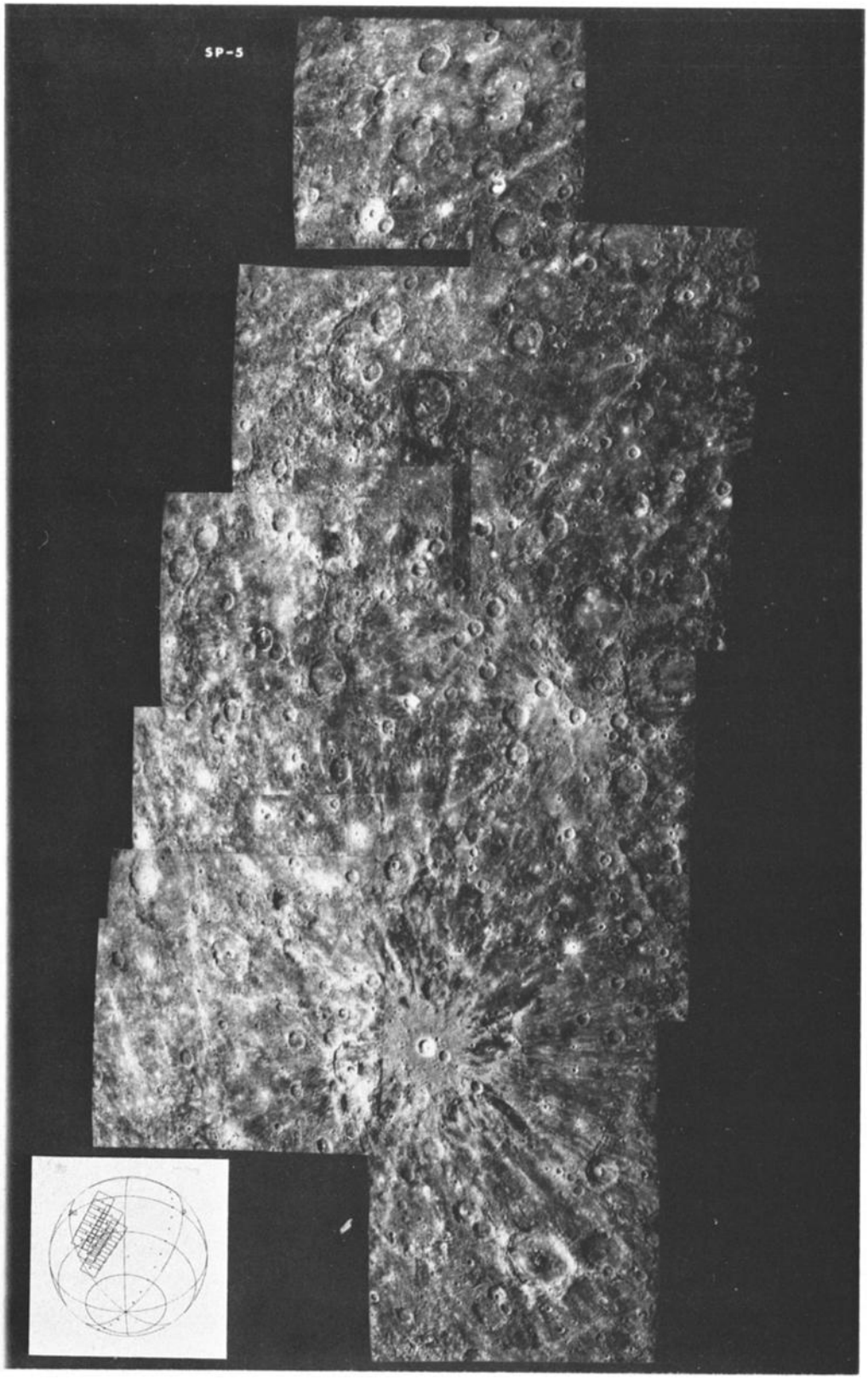

Fig. 9*e*

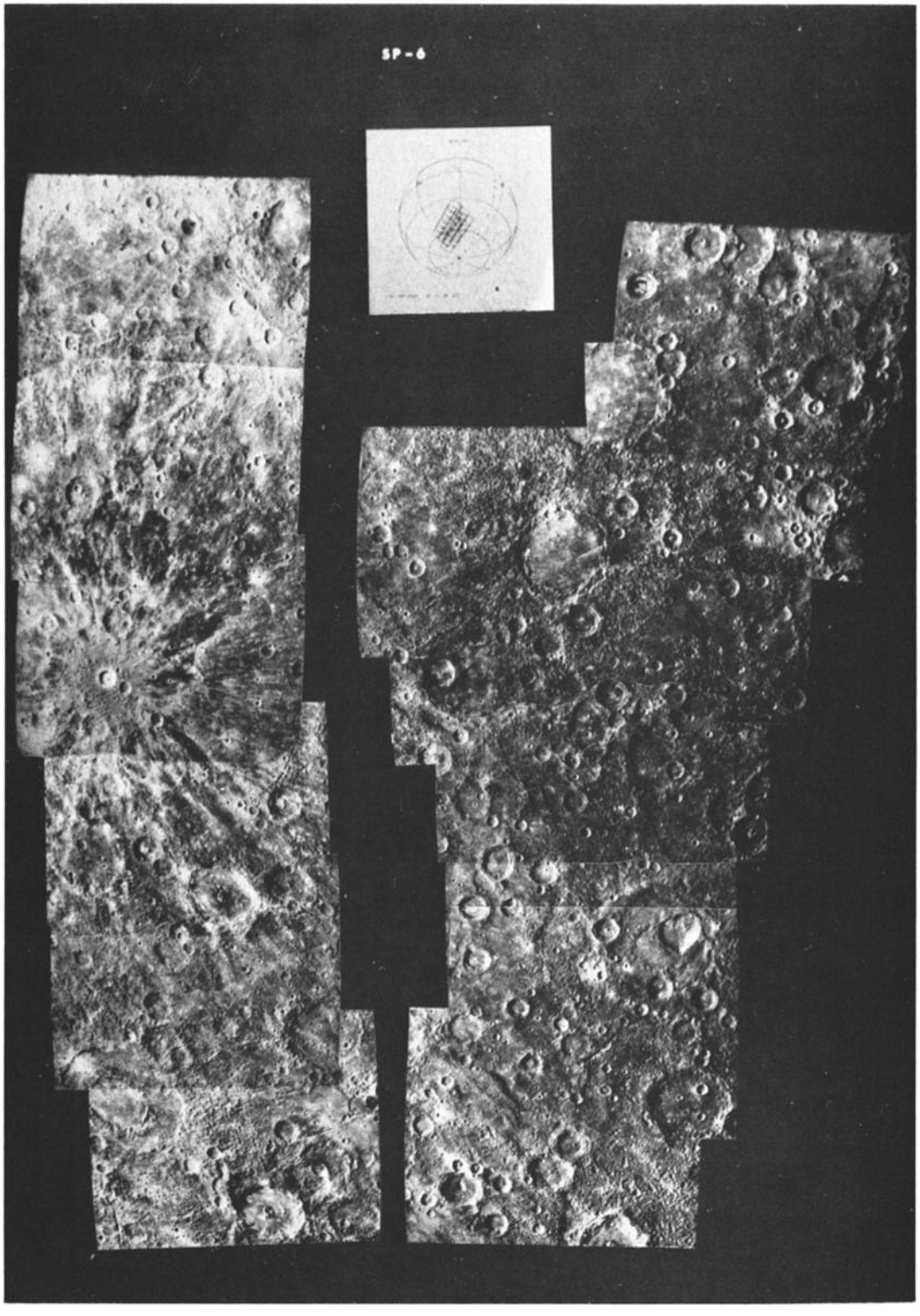

Fig. 9*f*

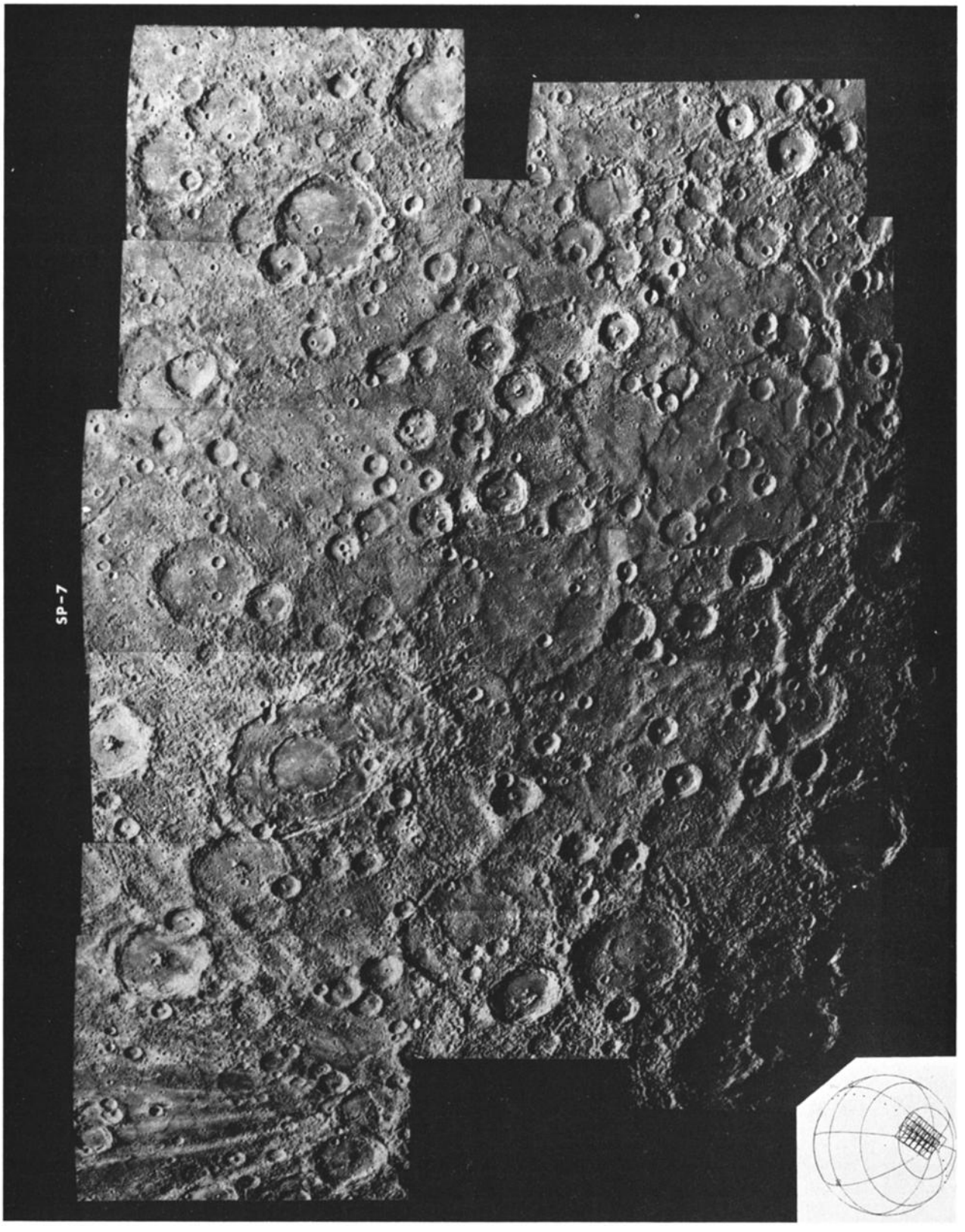

Fig. 9g

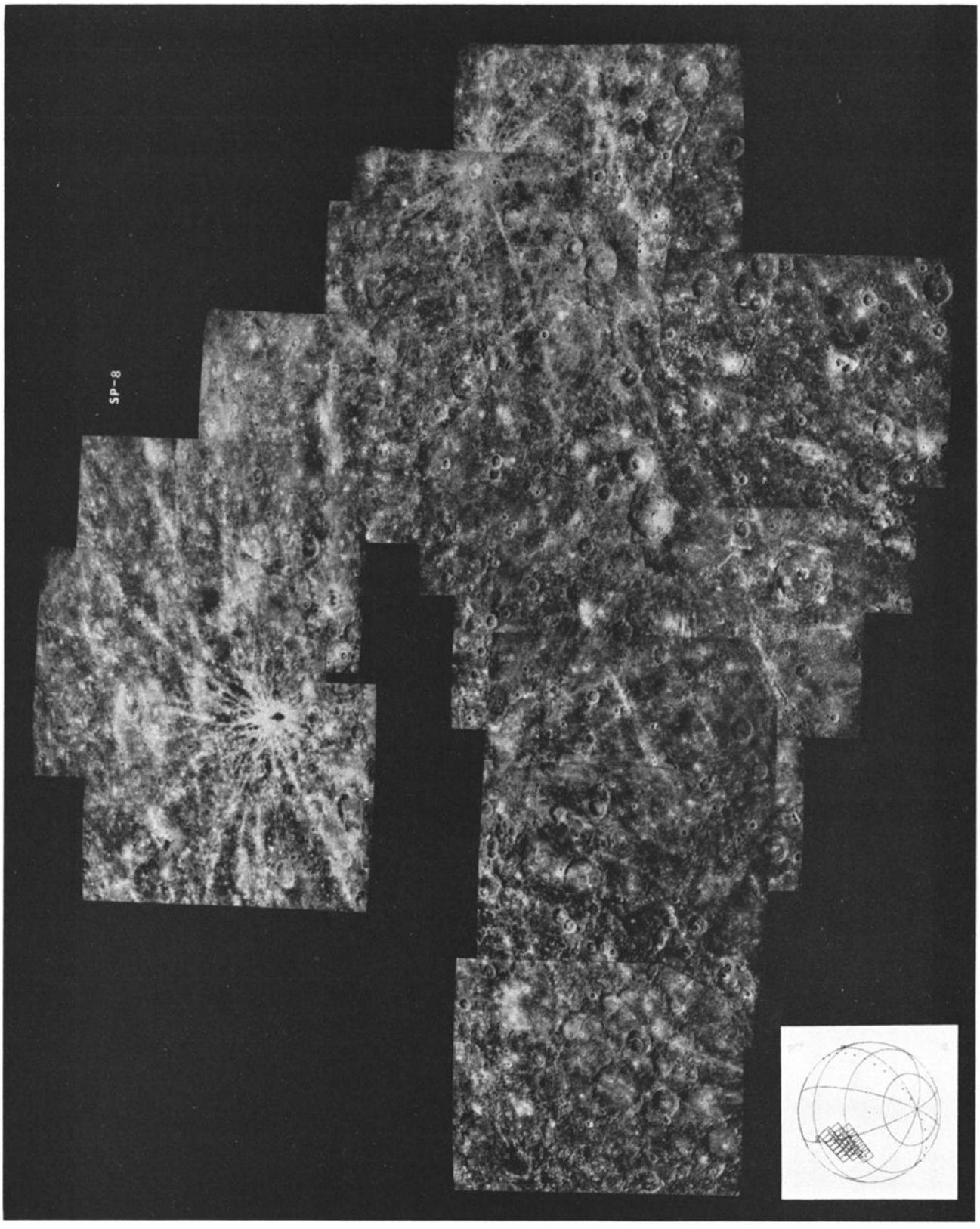

Fig. 9h

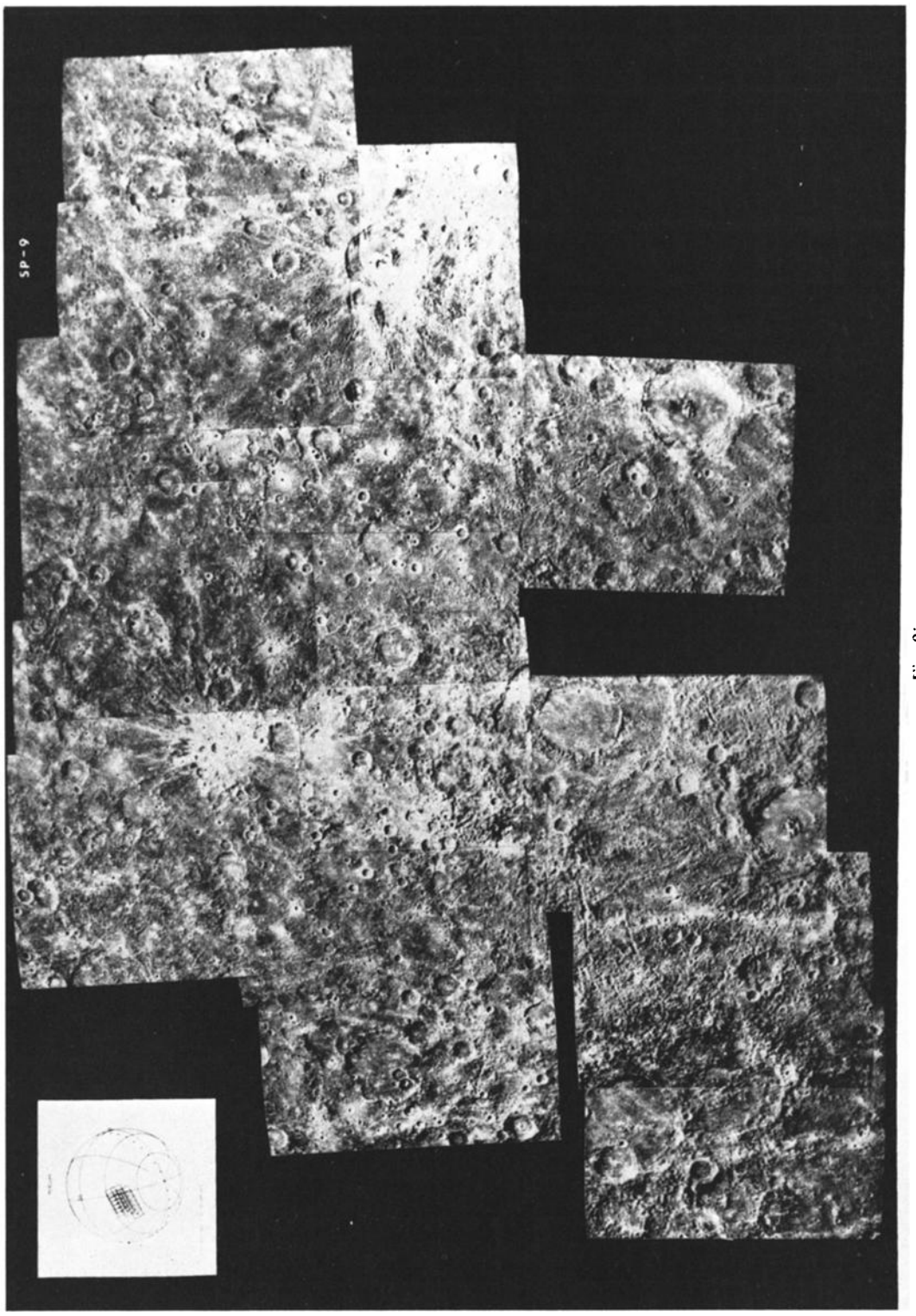

Fig. 9*i*

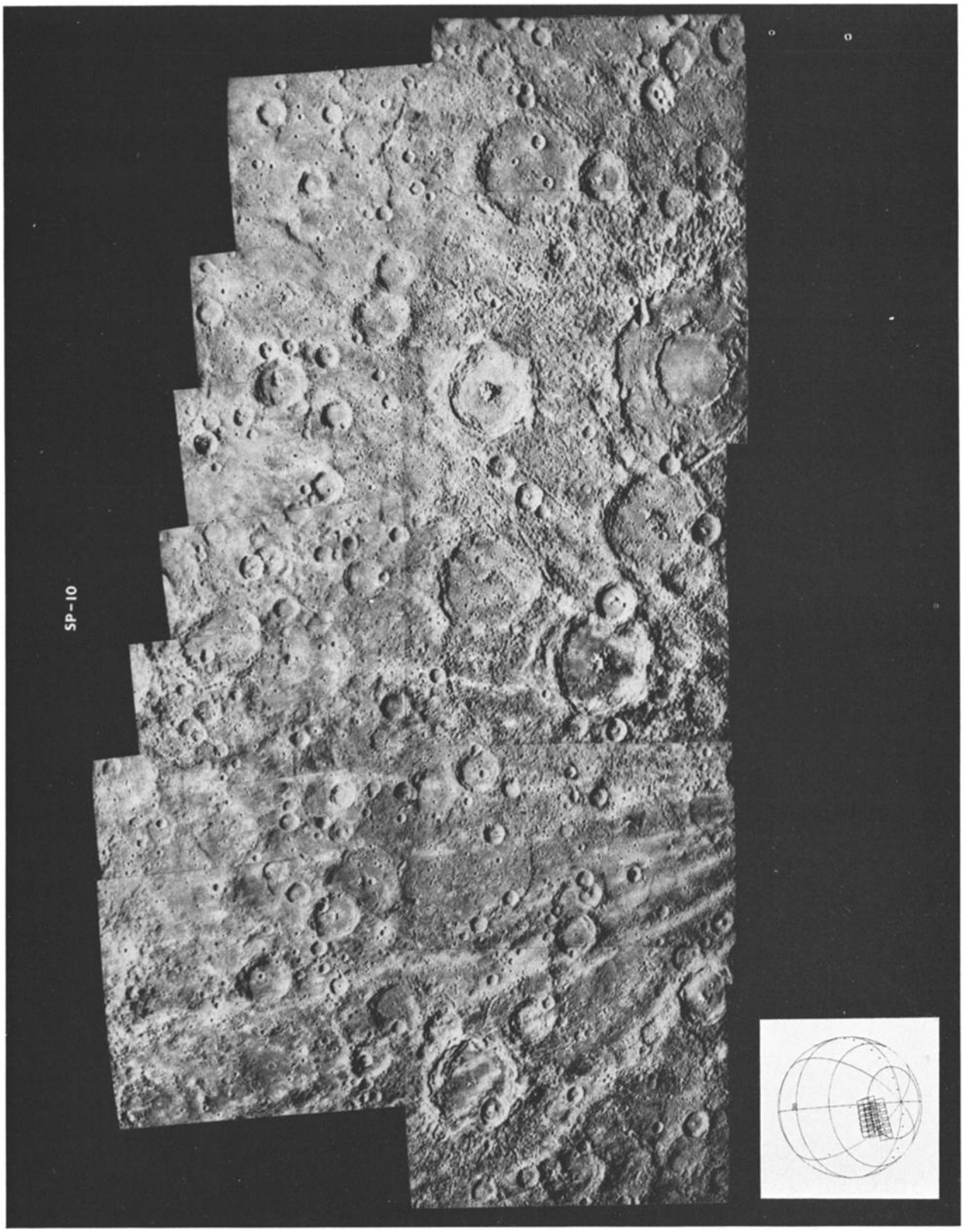

Fig. 9j

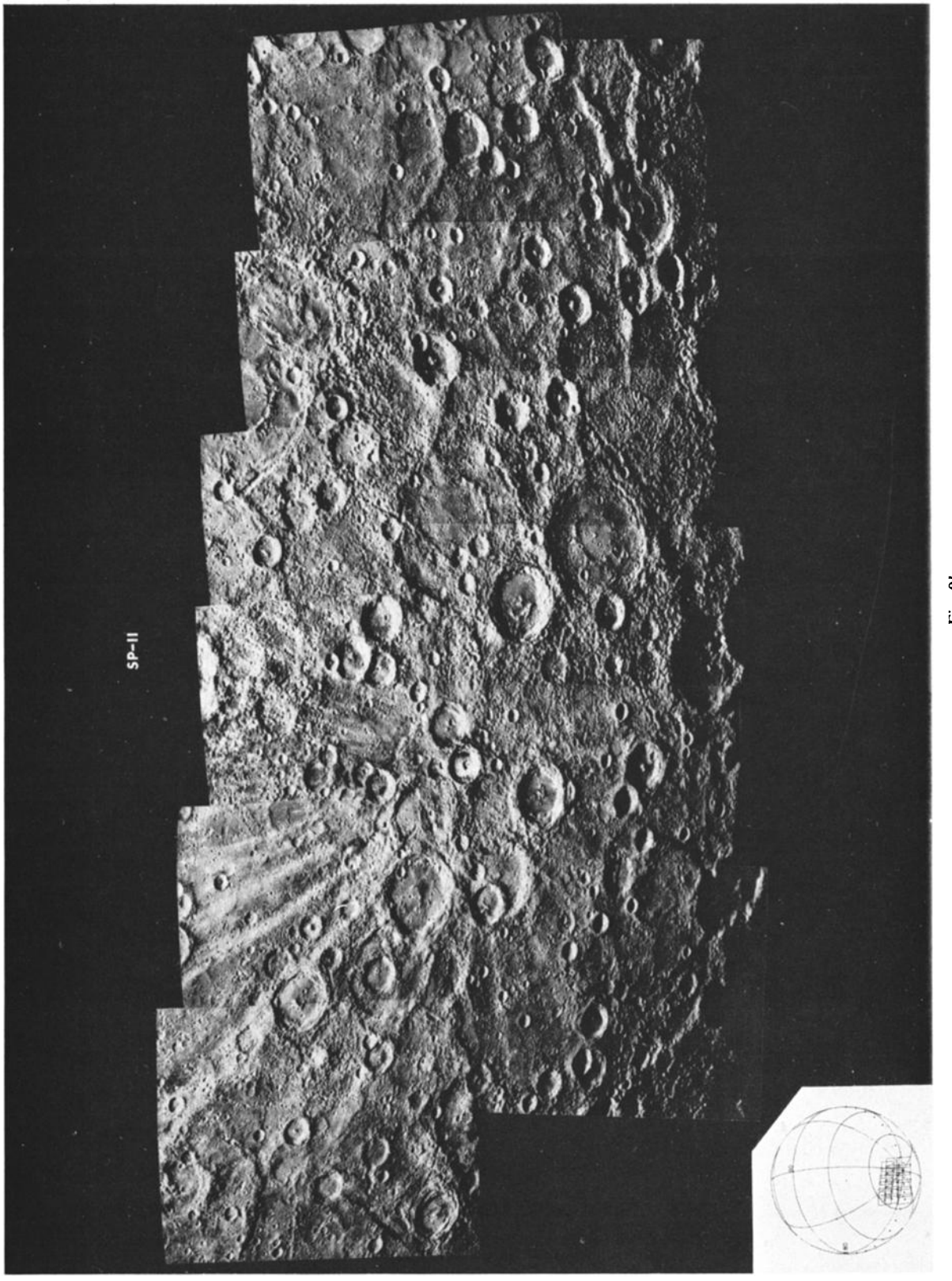

Fig. 9k

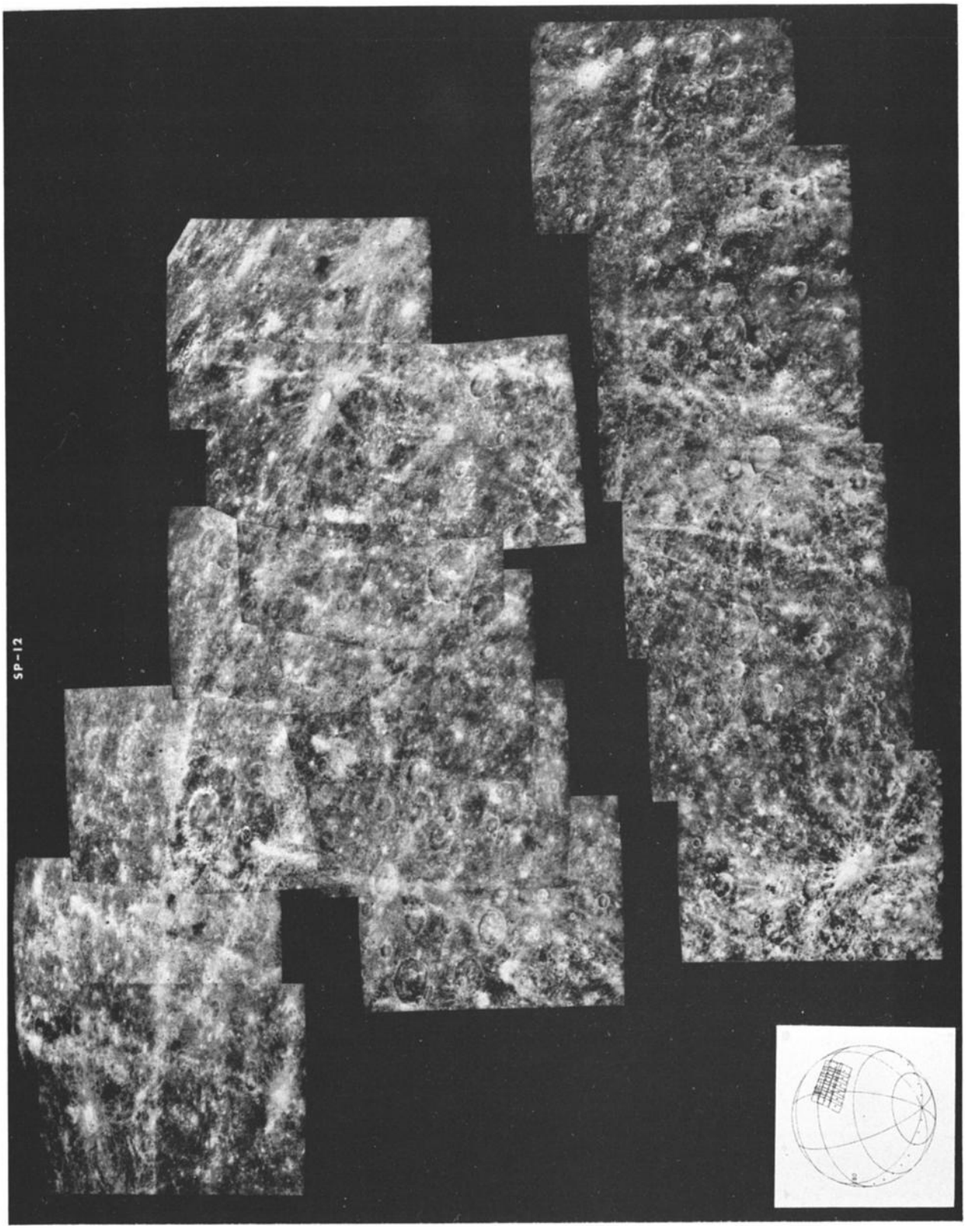

Fig. 9*l*

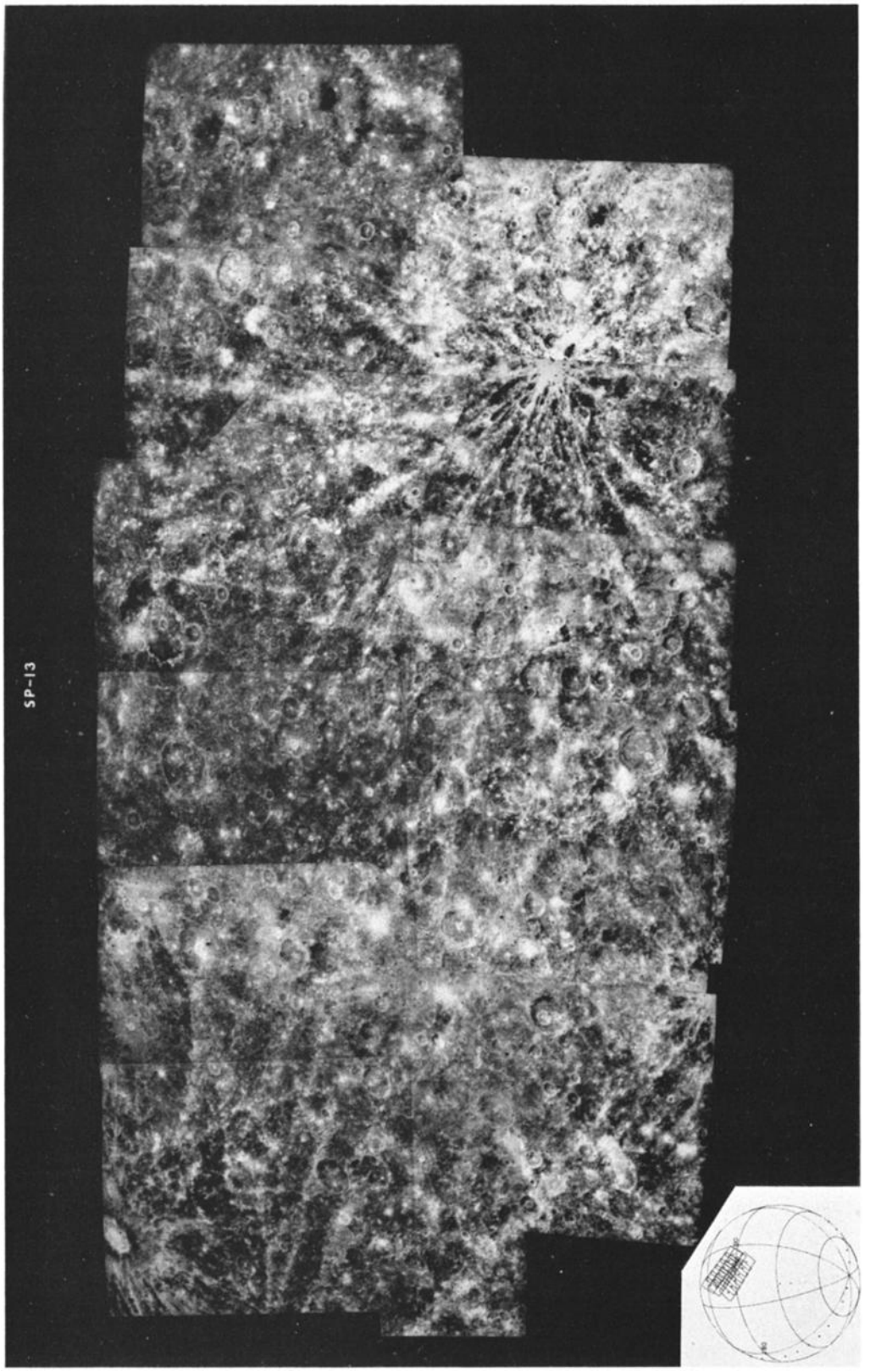

Fig. 9m

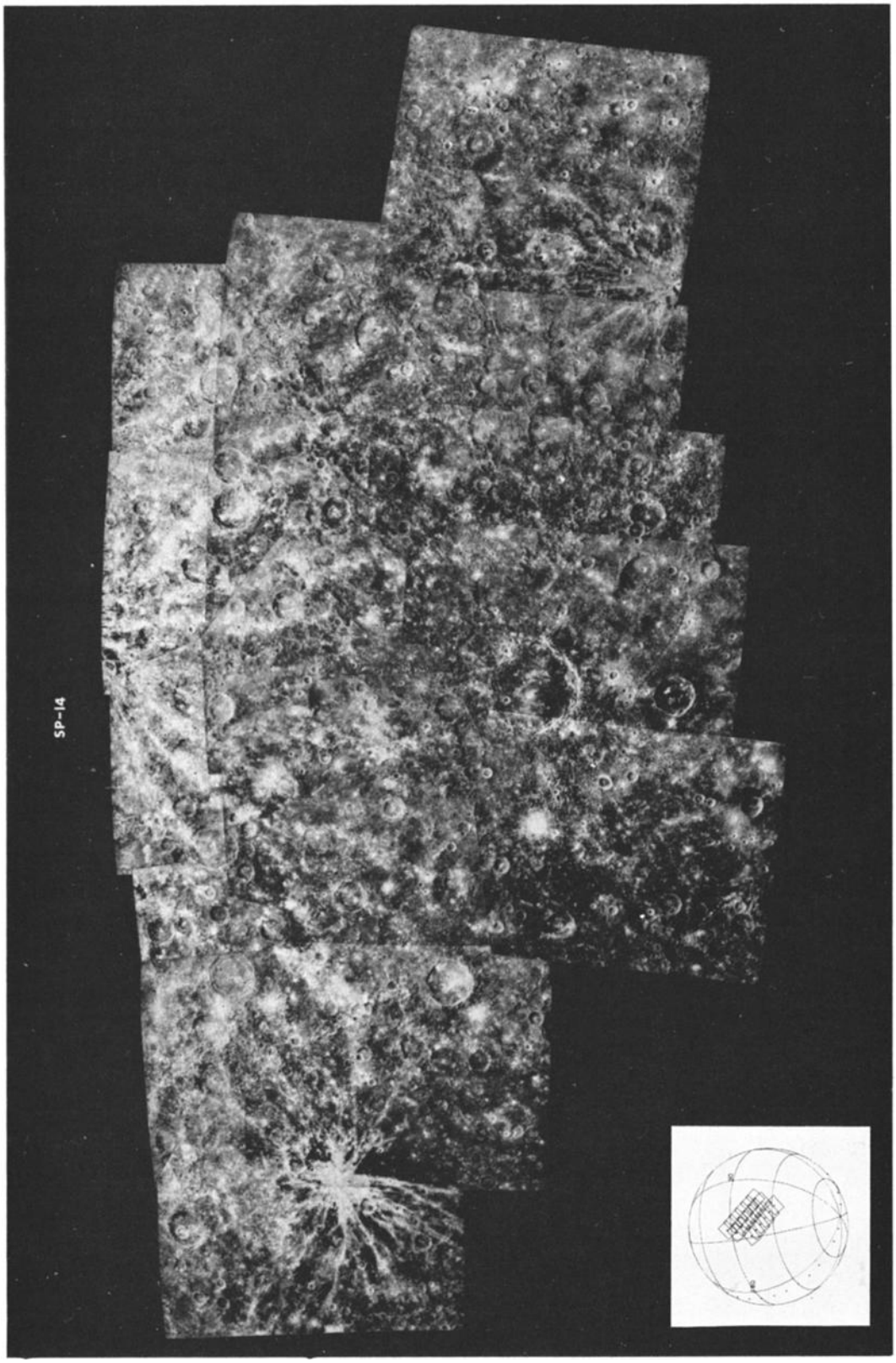

Fig. 9n

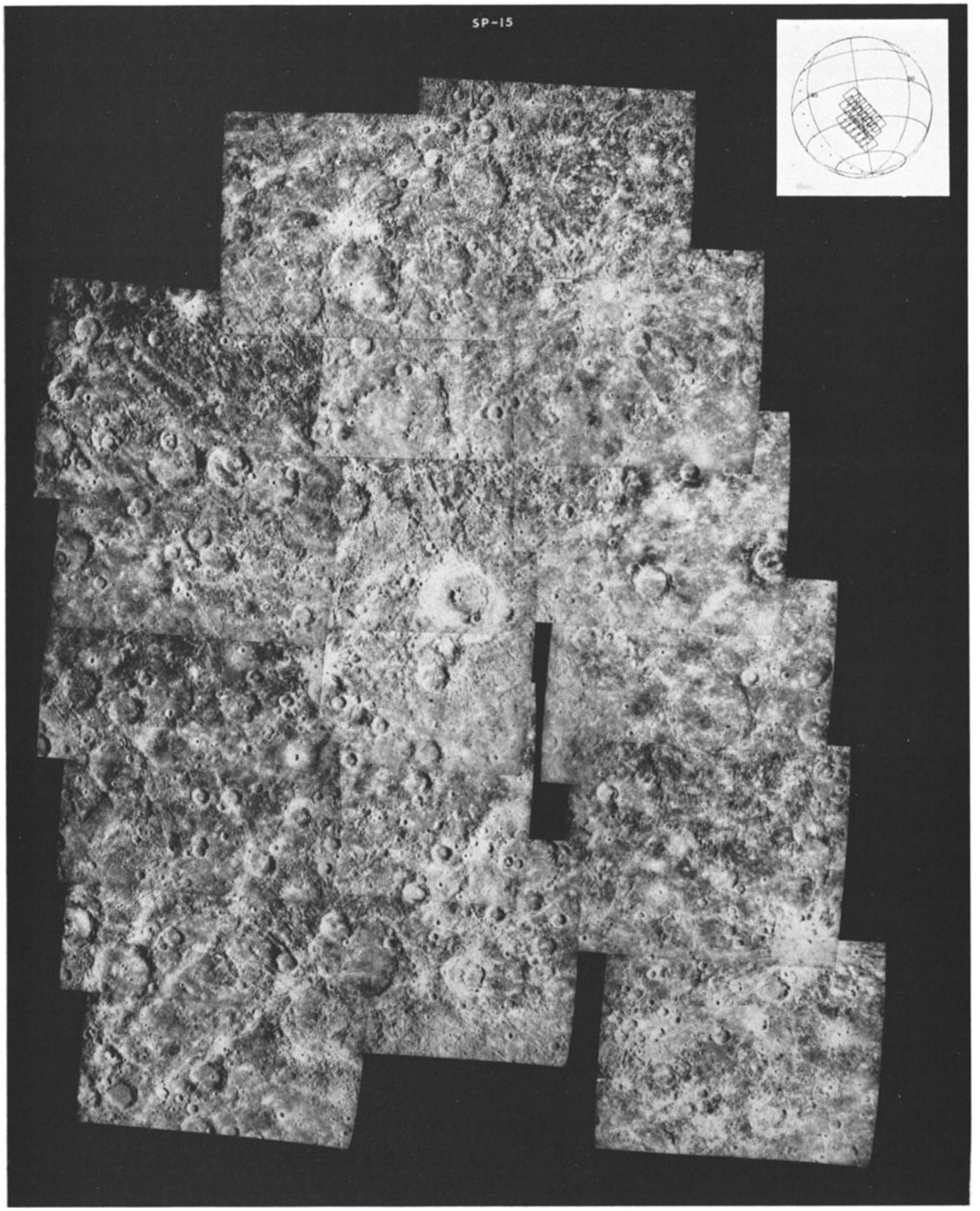

Fig. 9*o*

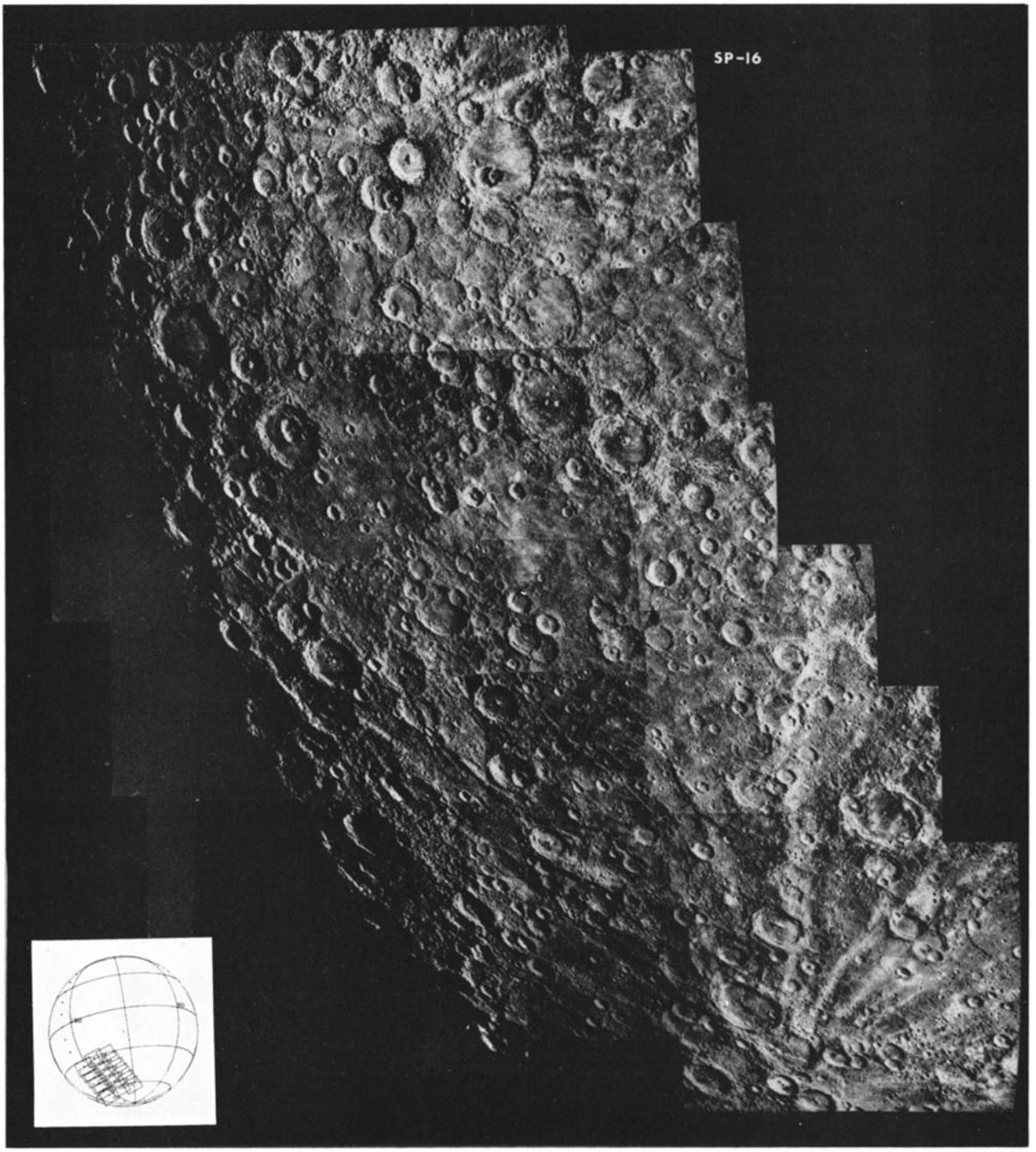

Fig. 9*p*

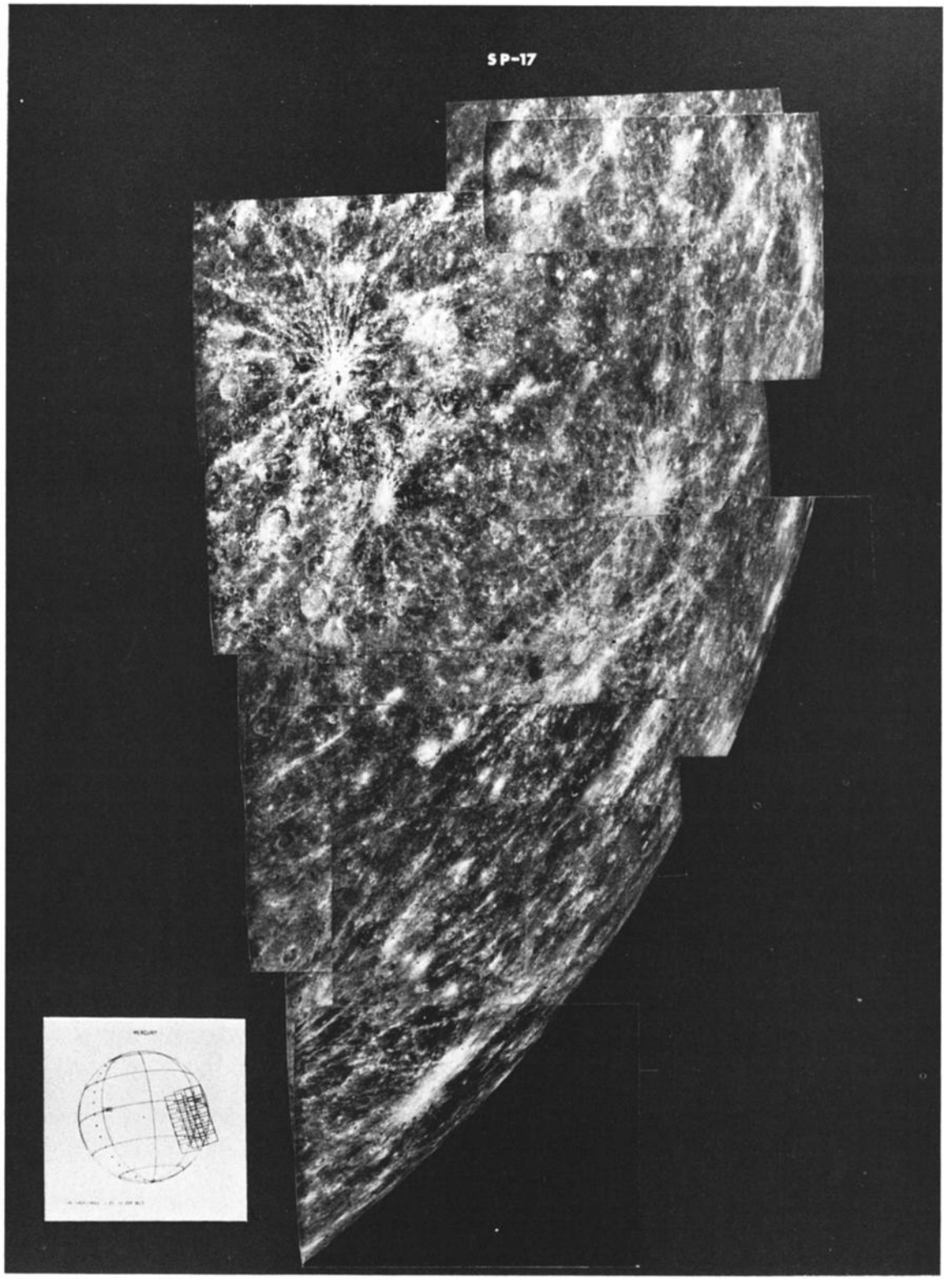

Fig. 9*q*

Fig. 9*r*

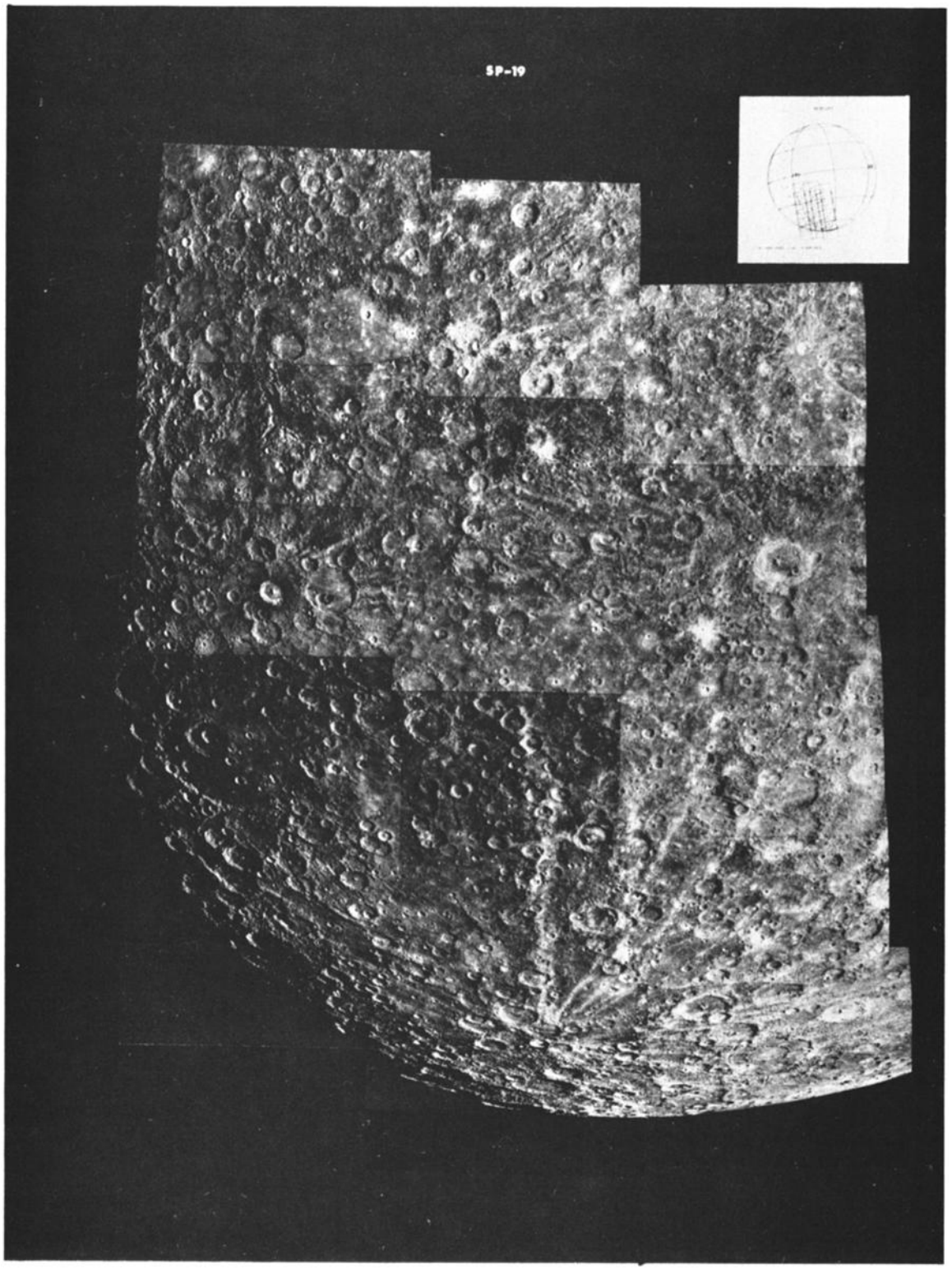

Fig. 9*s*

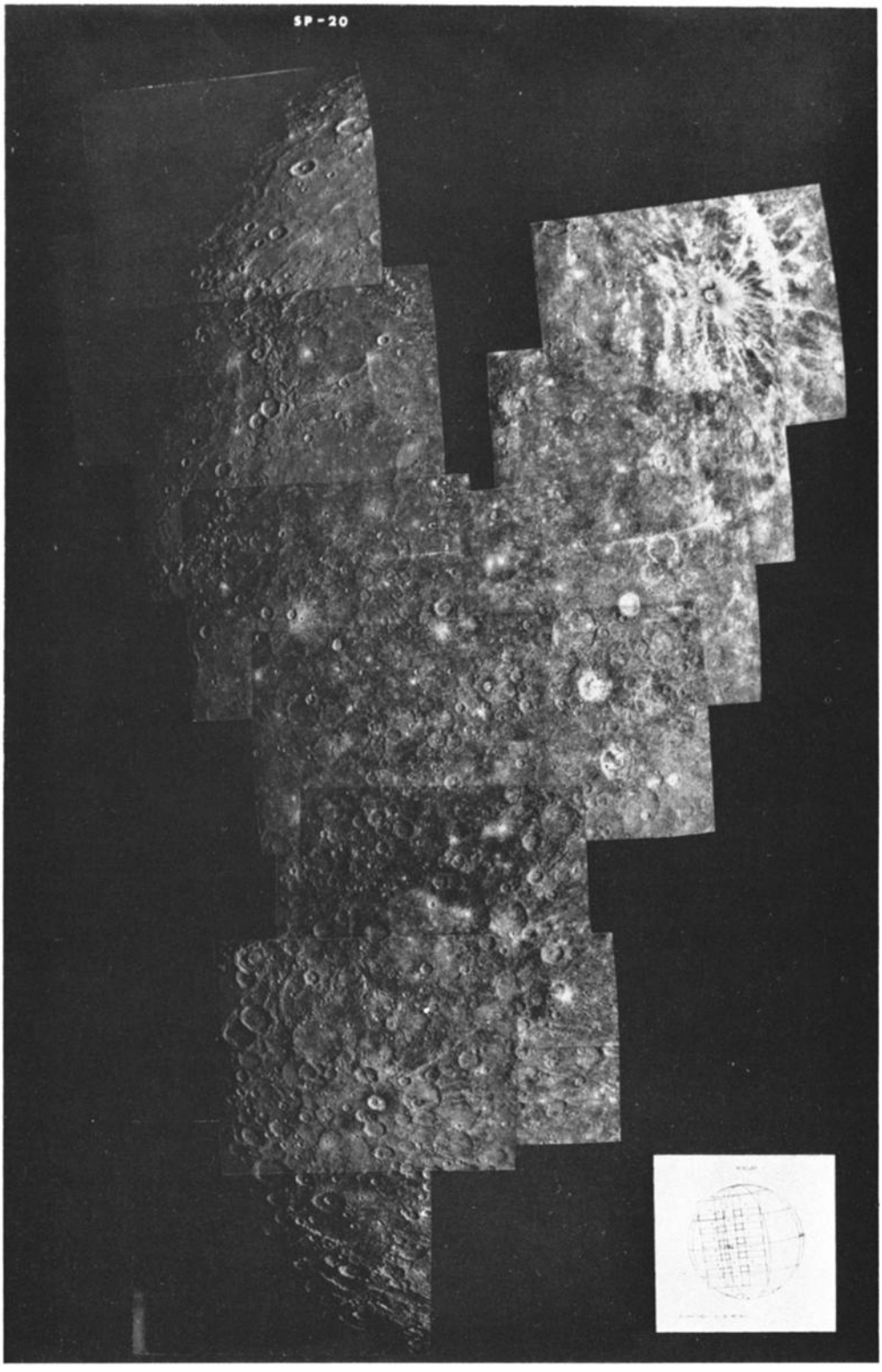

Fig. 9t

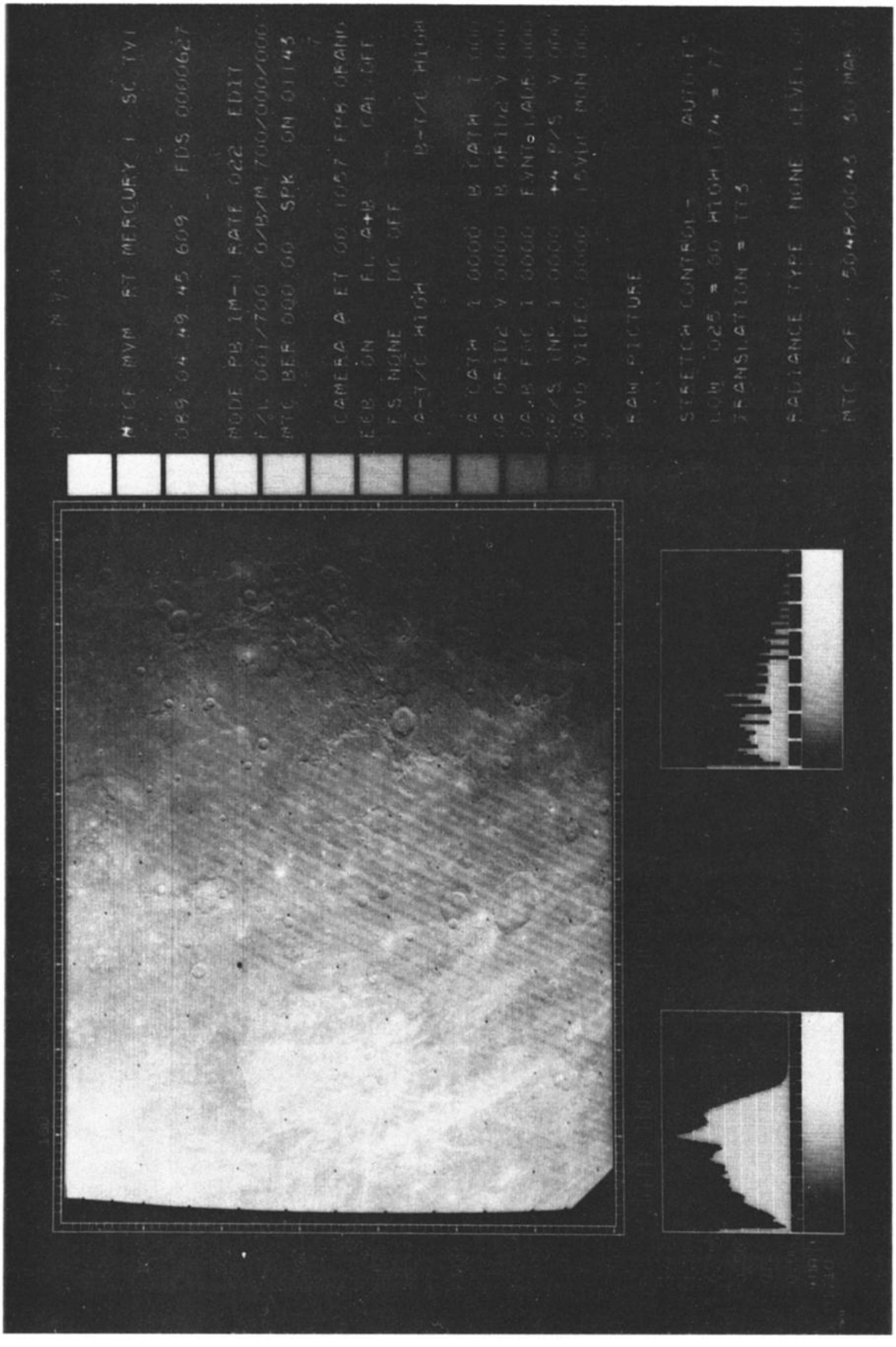

Fig. 10*a*

Fig. 10. Four picture versions of FDS 627. (*a*) Raw version of real-time processing. (*b*) Raw version of systematic processing. (*c*) High-pass-filtered version of systematic processing. (*d*) Vertical AGC-filtered version of systematic processing.

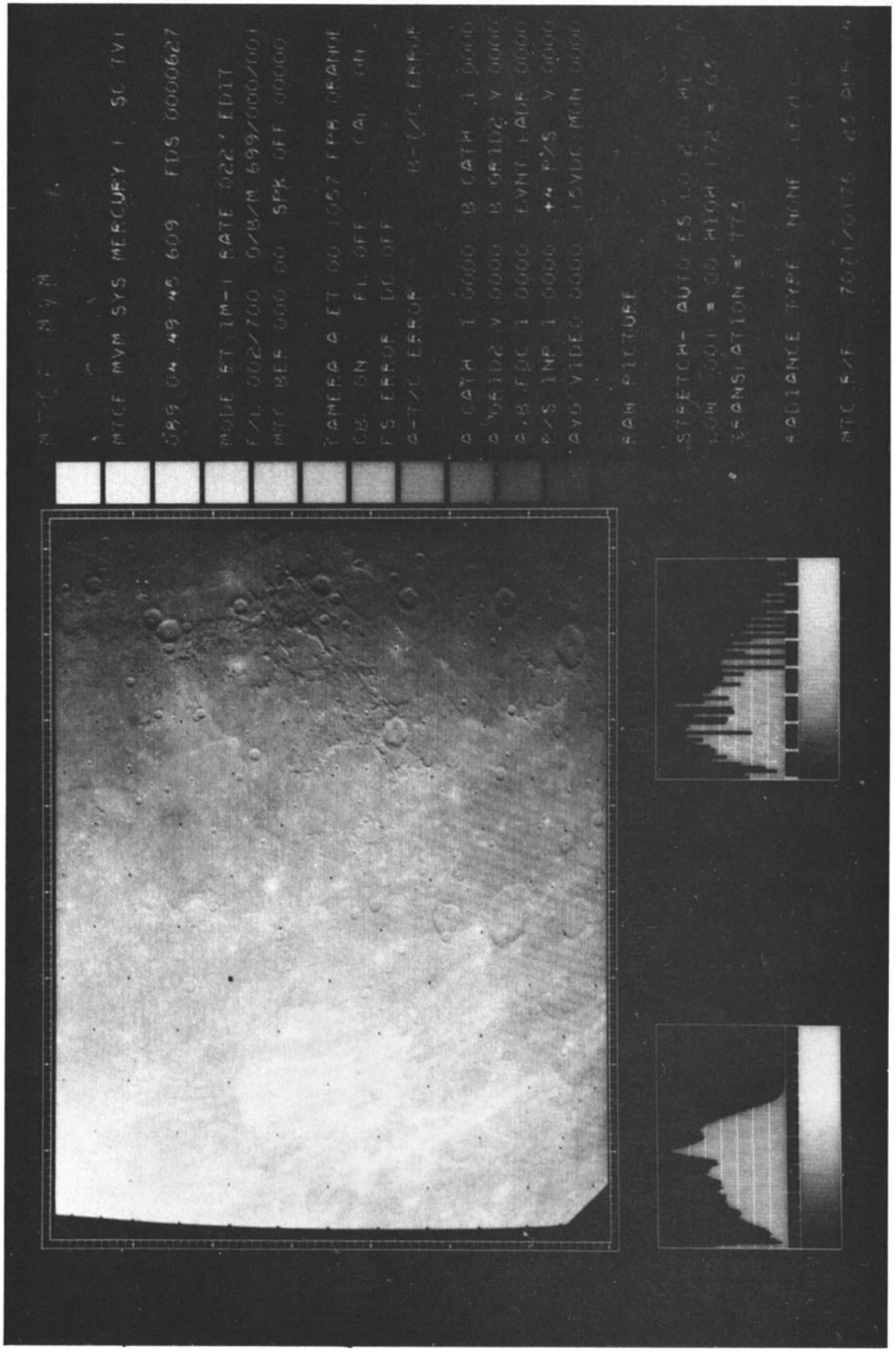
MTCF MVM SYS MERCURY 1 SC TV1
SCET 04 49 45 609 FDS 0000627
MODE ET 1M-1 RATE 022.7 EDIT
F/L 002/700 0/B/M 699/000/001
MTC BEE 000 00 SPK OFF 000000
CAMERA A ET 00 10:57 FRM GRAPHS
CB ON FL OFF CAL ON
FS ERROR DC OFF
B-T/C ERROR
A CATH 1 0000 B CATH 1 0000
A DEFLEC V 0000 B DEFLEC V 0000
A-B FOC 1 0000 EVNT LAPR 0000
P/S INP 1 0000 +4 P/S V 0000
AVG VIDEO 0000 TOTAL MEM 0000
RAM PICTURE
STRETCH- AUTO ES 10 62 ML
LOW 001 = 00 HIGH 172 = 67
TRANSLATION = 173
RADIANCE TYPE NONE LEVEL
MTC E/F 7071/0176 22 DES

Fig. 10b

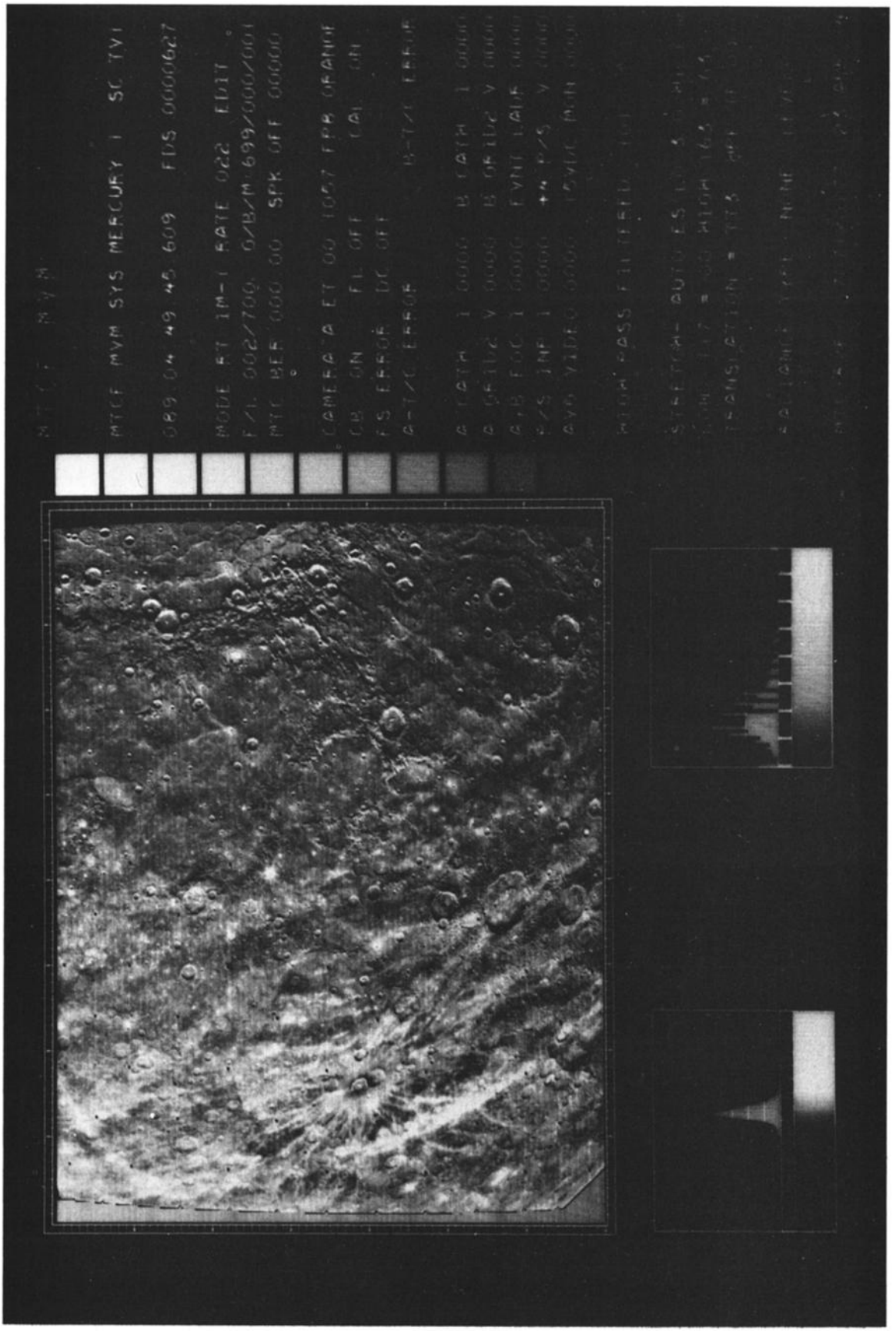
MTCF MVM SYS MERCURY 1 SC TV1
089 04 49 45 609 FDS 0000627
MODE ET 1M-1 RATE 022 EDIT
F/L 002/700. G/B/M 699/000/001
MTR REF 000 00 SPK OFF 000000
CAMERA-B ET 00 1057 FPB 0FAMNF
CB ON FL OFF CAL ON
FS ERROR DC OFF
B-T/C ERROR B-T/C ERROR

Fig. 10c

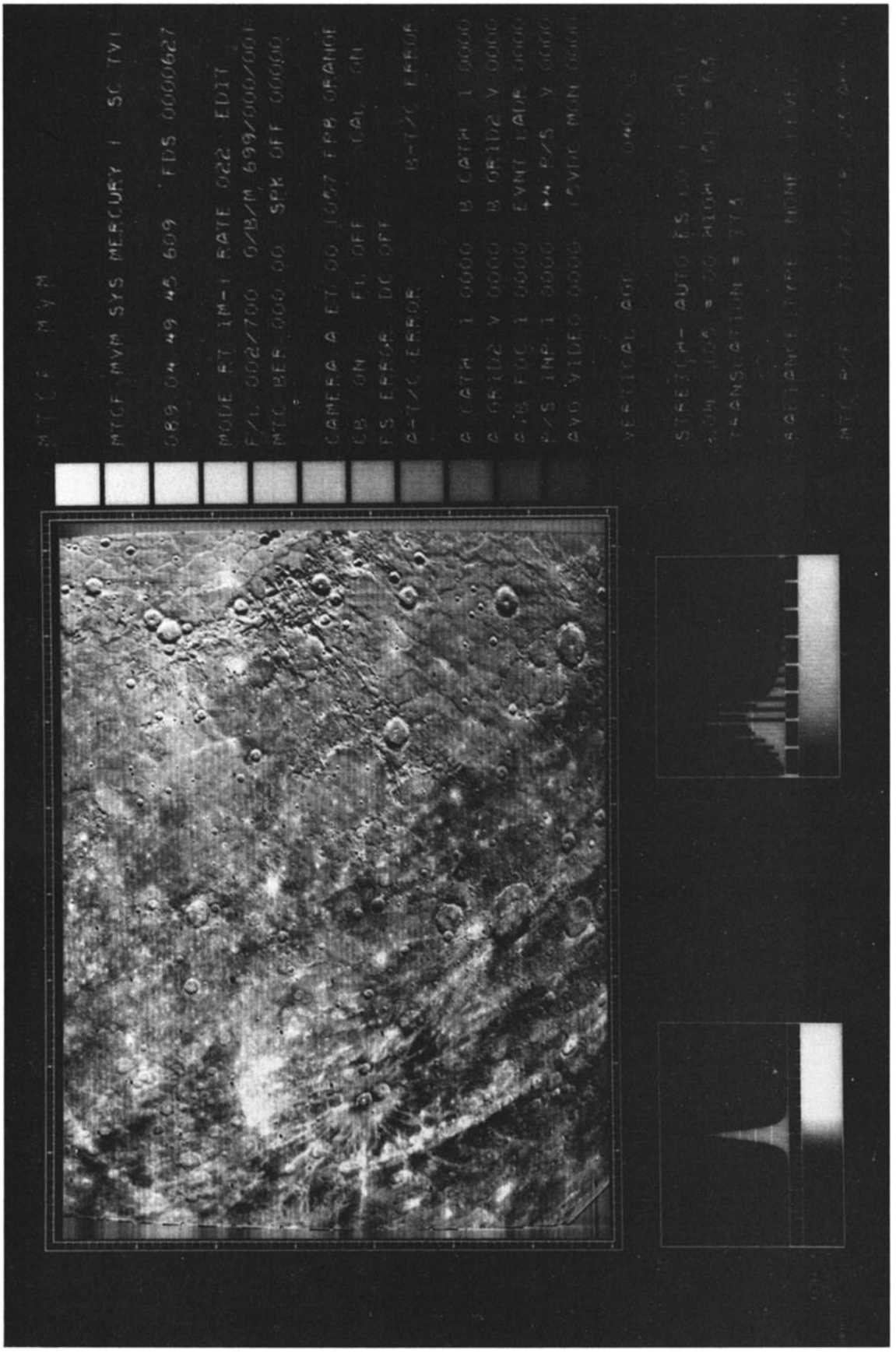
MTCF-MVM SYS MERCURY 1 SC TV1
089 04 49 45 609 FDS 0000627
MODE ET 1M-1 RATE 022 EDIT
F/L 002/700 G/B/M 699/000/001
MTC BER 000 00 SPK OFF 000000
CAMERA A ET 00 1057 FRM ORANGE
CB ON FL OFF CAL ON
FS ERROR DC OFF B-T/C ERROR
A CATH 1 0000 B CATH 1 0000
A GRID2 V 0000 B GRID2 V 0000
A-B FOC 1 0000 EVNT 1 AIR 0000
F/S INP 1 0000 +M F/S V 0000
AVG VIDEO 0000 CMIC MAIN 0000
VERTICAL OUT
STRETCH- AUTO ES
ZOOM 1.04 = 00 HIGH PAT = A2
TRANSLATION = 173
ROTATION = 000 MINF
MTF R/F

Fig. 10*d*

these changes was that much less information near planet limbs and frame sides or of low exposure values was destroyed by the automatic algorithms than would otherwise have been the case.

Examples of the processing described are shown in Figure 10. The frame shown covers much of the outgoing aspect of Mercury, from the limb in the lower left corner to very near the terminator in the lower right corner. Because of spacecraft-pointing geometry, north is down in frames taken after closest approach. The real-time and systematic contrast-enhanced raw pictures (Figures 10*a* and 10*b*) include a histogram of received data numbers labeled 'data input.' The histogram shows a wide range of values resulting from large lighting angle variations and significant albedo contrasts. This wide range of input values limits the degree of contrast enhancement possible without exceeding the dynamic range of the printing process. In this case the processing of these two raw versions differs only in details. High-pass-filtered and vertical AGC versions (Figures 10*c* and 10*d*) reduce regional contrast range while retaining local variations, thereby narrowing the width of the data input histogram and allowing a more effective contrast enhancement of fine details.

Acknowledgments. We are indebted to Nancy Evans, Patsy Conklin, and Isabel Lopez for their assistance in the preparation of the many pieces of art work and data tables. The planning and execution of the actual sequence were aided by software developed by Robert Toombs. We also thank Dave Theissen and the MVM '73 personnel in the Image Processing Laboratory at JPL for providing the photo products for the mosaics. This paper represents the results of one phase of research conducted at the Jet Propulsion Laboratory under NASA contract NAS 7-100. Division of Geological and Planetary Sciences, California Institute of Technology, contribution 2573.

REFERENCES

Clarke, V. C., Jr., and V. L. Evanchuk, 117.6 kilobit telemetry from Mercury, paper presented at 1974 International Telemetering Conference, Int. Found. for Telem., Instrum. Soc. of Amer., and Electron. Ind. Ass., Los Angeles, Calif., Oct. 15–17, 1974.

Cutts, J. A., Mariner Mars 1971 television picture catalog, vol. 1, Experiment design and picture data, *Tech. Memo. 33-385,* pp. 63–77, Jet Propul. Lab., Pasadena, Calif., 1974.

Dunne, J. A., Mariner 10 Mercury encounter, *Science, 185,* 141–142, 1974.

Dunne, J. A., W. D. Stromberg, R. M. Ruiz, S. A. Collins, and T. E. Thorpe, Maximum discriminability versions of the near-encounter Mariner pictures, *J. Geophys. Res., 76,* 438–472, 1971.

Larks, L., The narrow-angle telescope for the visual imaging subsystem of the Mariner Venus/Mercury (1973) spacecraft, *Proc. SPIE Instrum. Astron., 44,* 35, 1974.

McCord, T., and J. Adams, Mercury: Surface composition from the reflection spectrum, *Science, 178,* 745–746, 1972.

Rindfleisch, T. C., J. A. Dunne, H. N. Frieden, W. D. Stromberg, and R. M. Ruiz, Digital processing of the Mariner 6 and 7 pictures, *J. Geophys. Res., 76,* 394–416, 1971.

Young, A. T., Television photometry: The Mariner 9 experience, *Icarus, 21,* 262–282, 1974.

(Received February 12, 1975;
revised February 27, 1975;
accepted March 3, 1975.)